Defence Research and Development Canada
Recherche et développement pour la défense Canada

A Laboratory Study of Momentum and Passive Scalar Transport and Diffusion Within and Above a Model Urban Canopy – Final Report

T. Hilderman and R. Chong
Coanda Research & Development Corporation

Contract Scientific Authority: E. Yee, DRDC Suffield

Defence R&D Canada

Contract Report

DRDC Suffield CR 2008-025

December 2007

Canada

A Laboratory Study of Momentum and Passive Scalar Transport and Diffusion Within and Above a Model Urban Canopy – Final Report

T. Hilderman and R. Chong
Coanda Research & Development Corporation
110A – 3430 Brighton Avenue
Burnaby BC V5A 3H4

Contract Number: W7702-99R794

Contract Scientific Authority: E. Yee (403-544-4605)

Defence R&D Canada – Suffield

Contract Report

DRDC Suffield CR 2008-025

December 2007

Coanda
Research & Development Corporation

A Laboratory Study of Momentum and Passive Scalar Transport and Diffusion Within and Above a Model Urban Canopy - Final Report

for

Defence Research and Development Canada - Suffield

December 2007

CRDC00327

Prepared by:

T. Hilderman
R. Chong

110A - 3430 Brighton Ave., Burnaby, British Columbia, Canada, V5A 3H4
Tel: (604) 420-0367 Fax: (604) 420-0368 www.coanda.ca

Executive Summary

All dispersion tests were performed in Coanda's large re-circulating water channel (10 m long by 1.5 m wide by 1.0 m deep). Data were collected using laser doppler velocimetry (LDV) and laser induced fluorescence (LIF) techniques. Three urban obstacle array types were tested:

1. Raupach 2D tab array.
2. Mock Urban Setting Test (MUST) shipping container array.
3. Urban arrays based on cubical obstacles placed in a 2x2 unit cell.

Raupach 2D Tab Array

A staggered array of vertical stainless steel tabs 60 mm high by 10 mm wide by 1 mm thick were placed into acrylic panels in the bottom of the water channel. This array configuration was selected to provide a detailed data set that could be compared with results from a simulated plant canopy array constructed for wind tunnel testing by Raupach, Coppin and Legg (1986, Boundary-Layer Meteorology, 35:21-52).

The data set consists of:

- Vertical profiles of u, v, and w turbulent velocity statistics at 19 positions within a unit cell. Each data point is a 500 second LDV sample.
- 70 linescan concentration measurements at 1000 simultaneous points along lines horizontally and vertically through the plume. Spatial resolution was 1 mm with samples collected at 300 Hz for durations of 2000 seconds.
- Qualitative 2D planar concentration measurements at 7 downstream positions.

MUST Array

The Mock Urban Setting Test (MUST) array was tested as part of a larger project by the Technical Cooperation Programme (TTCP) Chemical and Biological Defence (CBD) Group, Technical Panel 9 (TP-9). Several countries cooperated to compare the results obtained from measurements in the same urban obstacle array at different scales in different experimental configurations. The full scale case was tested in the fall of 2001 at the Dugway Proving Grounds in Utah with a 10x12 array of shipping containers. Wind tunnel tests were

completed at Monash University in Australia at approximately 1:50 scale. Water channel tests were performed by Coanda at 1:205 scale.

The data set contains:

- Vertical profiles of u, v, and w velocity statistics at 16 positions throughout the array and 11 points around a single obstacle at the centre of the array.
- 130 horizontal and vertical linescan concentration profiles with 1000 second duration, 300 Hz samples. Configurations included two source positions within the array and comparison cases without obstacles or surface roughness.
- 32 series of 100 puff releases measured along horizontal and vertical lines.
- Qualitative 2D planar concentration measurements at 4 downstream positions.

Coanda's experimental capabilities were validated by very favorable comparisons between the full scale MUST tests and the water channel data set.

Urban Arrays

The third array type tested was an idealized urban array, constructed with a combination of Lego™ blocks and machined acrylic blocks. These tests considered the effect of obstacle height, obstacle position, and source position relative to the obstacles. The base obstacle was a cube of 1 unit dimension (31.75 mm=1.25") placed into one quadrant of a unit cell which was 2 units x 2 units square. Arrays were constructed by stacking and arranging these unit cells and cubical obstacles.

The data set contains:

- 38 obstacle array configurations.
- 570 linescan concentration measurements of 1000 seconds duration at 300 Hz sampling rates at various horizontal and vertical positions of interest within the arrays. Some arrays were tested at 30° or 45° angles to the approach flow.
- Velocity measurements at selected locations of interest in 9 of the 38 array configurations.

Documentation

This final report document describes the experimental configurations, presents sample figures illustrating the type of data available and contains Appendices detailing the data formats. An accompanying set of data CD's contains:

- Electronic copies of expanded supplementary reports for each data set. Each supplementary report has a more detailed description of the reduced data files included on the CD's and more complete sets of figures.
- Reduced data in the form of Microsoft Excel spreadsheets (`*.xls`) and comma separated variable (`*.csv`) ASCII text files.

- Plot files in the Origin project format (`*.OPJ`).

Raw data files of velocity and linescan concentration measurements are available for further analysis.

Further Information

Enquires related to the UDM data set or requests for copies should be directed to:

Dr. Trevor Hilderman
Coanda Research & Development Corporation
110A - 3430 Brighton Avenue
Burnaby, British Columbia
Canada, V5A 3H4
Phone: (604) 420-0367 x229
Fax: (604) 420-0368
E-mail: `trevor_hilderman@coanda.ca`
Web Page: `www.coanda.ca`

or

Dr. Eugene Yee
Defence Research and Development Canada - Suffield
Department of National Defence
P.O. Box 4000
Medicine Hat, AB
Canada, T1A 8K6
Phone: (403) 544-4605
E-mail: `Eugene.Yee@drdc-rddc.gc.ca`

Disclaimer

Coanda Research & Development Corporation shall not be liable for any direct, consequential or any other damages resulting from the use of the UDM data. Coanda assumes no responsibility for the accuracy of the UDM data; for statements or errors and omissions in the documentation; or for the use of this material in whole or in part by any person or agency.

Contents

List of Figures

1 Project Description

The objective of the UDM project was to collect extensive data sets of dispersion through groups of obstacles to assist in the development and validation of models of urban dispersion. Both turbulent velocity measurements and scalar concentration data were collected in three different urban obstacle arrays constructed in Coanda's re-circulating water channel:

1. Raupach 2D tab array.
2. Mock Urban Setting Test (MUST) shipping container array.
3. Urban arrays based on cubical obstacles placed in a 2x2 unit cell.

In all cases, the water channel was configured to simulate a rough-surface turbulent atmospheric boundary layer under neutrally stable conditions. Scalar releases were all performed with low momentum sources and neutrally buoyant fluorescent tracer solutions.

The remainder of this report discusses the details of the experiments and provides a brief overview of the data collected. The Appendices give the technical details on the velocity and concentration statistics that were calculated as well as the arrangement of information in the data files.

2 Coanda's Experimental Facilities

The main piece of experimental apparatus used in the UDM project study was Coanda's re-circulating water channel, shown in Figure 1. The channel has a glass bottom and sides with a minimum number of support braces to maximize optical access to the test section as can be seen in Figures 1 and 2. The specifications of the channel are:

- Maximum Flow Rate = 8.5 m^3/s driven by a 30 Hp centrifugal pump
- Plenum Dimensions = 2.4 m high by 2.4 m wide by 2.4 m long
- Channel Test Section = 1.0 m deep by 1.5 m wide by 10 m long

The coordinate directions used for all measurements follow the typical meteorological standard as shown by the coordinate axes superimposed on the photograph in Figure 1(b).

- x is positive in the direction of the flow.
- y is positive to the left if looking in the positive x direction.
- z is positive in the upward direction.

The inlet plenum is on the left side of the photographs in Figure 1. The edge of the outlet plenum can be seen on the right hand side of the photographs. Water is pumped from the outlet plenum through external PVC piping and into the inlet plenum through a distribution header.

Flow enters through the header in the bottom of the plenum, passes through a flow straightener, then up through two sets of turning vanes. There is a smooth contraction to the width and depth of the channel test section and an additional flow straightener at the inlet to the test section. The plenum is large so that the velocities are small to ensure there are no uncontrolled secondary flow patterns developed in the plenum that can be transferred into the test section. Figure 3(a) shows the top of the inlet plenum with the flow straighteners and contraction.

After the contraction and final flow straightener there was an array of square bars and a "saw-tooth" trip fence, shown in Figure 4. These flow conditioning elements promoted the generation of medium to large scale turbulence and encouraged the rapid development of the desired turbulent boundary layer velocity. The water depth was controlled by an adjustable weir in the outlet plenum shown in Figure 3(b).

The obstacle arrays tested in the UDM study were placed on the bottom of the channel. For each array configuration, the inlet flow conditioning elements were adjusted and modified to ensure that there was a well-developed turbulent boundary layer at the array location between approximately 5 and 8 m down the channel. Only neutrally stable atmospheric conditions were simulated.

A computer controlled traverse mechanism and various support structures were built on top of and around the channel for the experiments. For example, Figure 1(a) has the black 3-axis traverse frame in the foreground on the right side of the image. Figure 1(b) shows the same 3-axis traverse mounted on top of the channel along with a framework of

aluminum extrusions shown on the right side of the image. All of these components were used to support cameras, laser optics, and velocity measurement probes as required for each experiment.

2.1 Laser Doppler Velocity Measurements (LDV)

Velocity data were collected with a 4 beam 2-component TSI fiber optic laser doppler velocimeter (LDV) powered by an argon-ion laser. Titanium dioxide particles were used as seed particles. Figure 5 shows three views of the LDV probe and the laser beams coming out of the probe.

The LDV data were collected with 500 second sample times for each position. The data rate for the LDV measurements depended upon the flow velocity, particle seeding density, and optical properties of the lenses, but was typically 50-500 Hz.

The measurement volume at the crossing point of the LDV beams ranged in size from 90 μm diameter by 1.3 mm long for the 350 mm focal length lens, to 125 μm diameter by 2.5 mm long for the 500 mm focal length lens. The choice of lens depended on the desired measurement position relative to the probe position. For measurements through the surface of the water, a small window, seen at the top of Figure 5(b) and 5(c), was suspended on the water surface to eliminate ripples which would distort the beams.

To get better measurements at ground level in the arrays, the LDV probe was tipped by up to 5 degrees from the horizontal. Figure 5(c) shows the beams tipped and bouncing off a mirror to make uw component measurements from above. In these cases, the vertical component w that was measured was actually a few degrees off from the true vertical. This small error was insignificant because the cross-stream average velocity v was zero and the w and v turbulent components were nearly identical in magnitude.

2.2 Scalar Concentration Data

Laser induced fluorescence (LIF) techniques were used to measure the concentration of dispersing dye tracer within the obstacle arrays. Sodium fluorescein dye was illuminated by an argon-ion laser beam or light sheet and the fluorescent intensities were measured with CCD cameras. The fluorescence intensity was a function of the dye concentration, the incoming light intensity, and the attenuation of light through the dye.

Fluorescein has a molecular diffusivity of $D = 5.2 \times 10^{-10}$ m^2/s. With a kinematic viscosity of water of $\nu = 1.0 \times 10^{-6}$ m^2/s, the Schmidt number ($Sc = \nu/D$) for the dye was 1920. The dye source concentration was adjusted to ensure optimal measurements at all downstream positions. All releases were neutrally buoyant.

2.2.1 1D Linescan LIF

The majority of the concentration data were collected with the 1-D LIF linescan system illustrated in Figure 6(a). Fluorescent dye was released from the source and illuminated at a single downstream position with a laser beam from an argon-ion laser. A Dalsa monochrome digital linescan CCD camera (1024x1 pixels), 12-bit (4096 gray levels), measured the intensity

of dye fluorescence at 300 lines per second. The total sample time for each position was typically 1000 seconds, producing time series of 300,000 samples at each measured pixel. The pixel spatial resolution was between 0.5 and 1 mm depending on the positioning of the camera and laser line. In addition to the horizontal linescan measurements depicted in Figure 6(a), vertical linescans were made by swapping the positions of the laser beam and the camera so that the measurement line was oriented along the z axis.

The large data sets collected via linescan have excellent time and spatial resolution. This enables concentration fluctuations, probability distributions of concentration at a point, concentration frequency spectra and other higher order statistical moments of concentration to be evaluated. Even the highly intermittent edges of the plume can be resolved. In addition, the simultaneous sampling of more than 1000 points across the plume enables cross-correlations between different spatial positions to be evaluated. There are currently no other experimental techniques that can provide this quality of data.

2.2.2 2D Area Scan LIF

Along with the 1D linescan, some measurements were made with a 2D LIF system as shown in Figure 6(b). The dye was illuminated by a laser light sheet created by a Powell lens and measured with a Hitachi monochrome analog CCD camera (640x480 pixels) digitized with an 8 bit (256 gray levels) A/D at 30 frames per second. A limited number of data sets were collected to provide some quantitative and excellent qualitative images of plume structure.

2.3 Calibration and Processing

Both of these LIF measurement systems were calibrated in-place each day at a range of dye concentration levels. The calibration accounted for pixel to pixel variation in the cameras, variations in laser beam intensity, and non-uniformity in the 2D light sheet. Raw image intensity data were collected on hard disk for the duration of the experiments. Post-processing was performed on the intensity data to apply the concentration calibration for each pixel, remove background levels which built up in the channel as fluorescent dye was released, and to correct for the effect of laser light attenuation through the dye. All post-processing methods and software were developed by Coanda personnel.

(a)

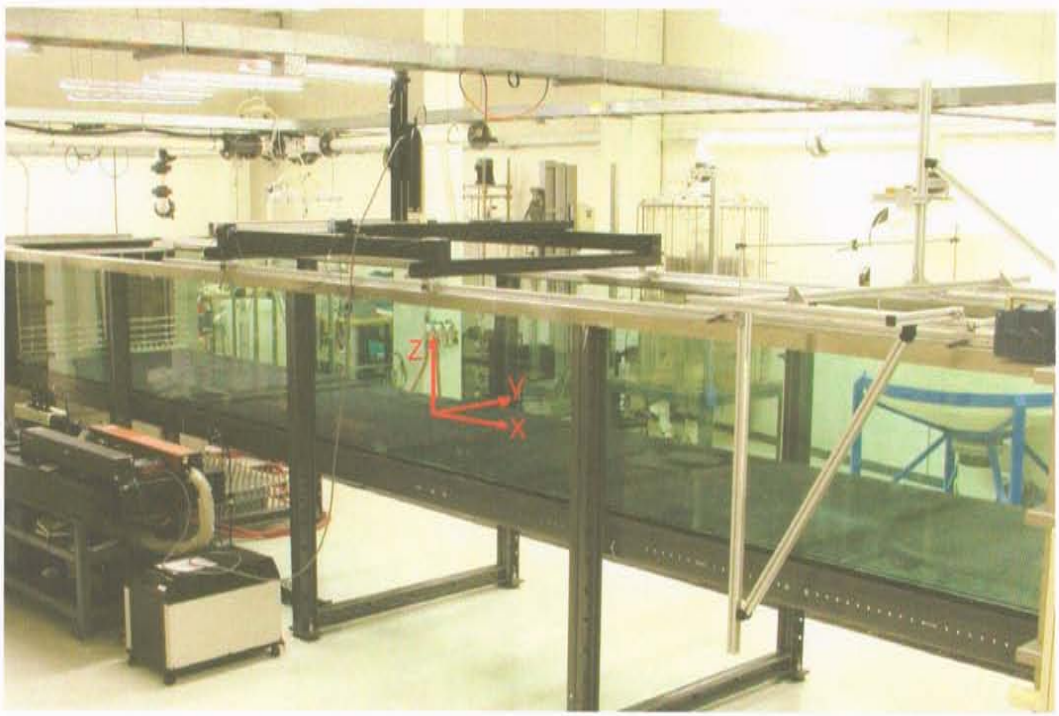

(b)

Figure 1: (a) Overall view of Coanda's water channel with the Raupach array installed. (b) View of water channel with the expanded metal roughness and coordinate system superimposed on the photograph.

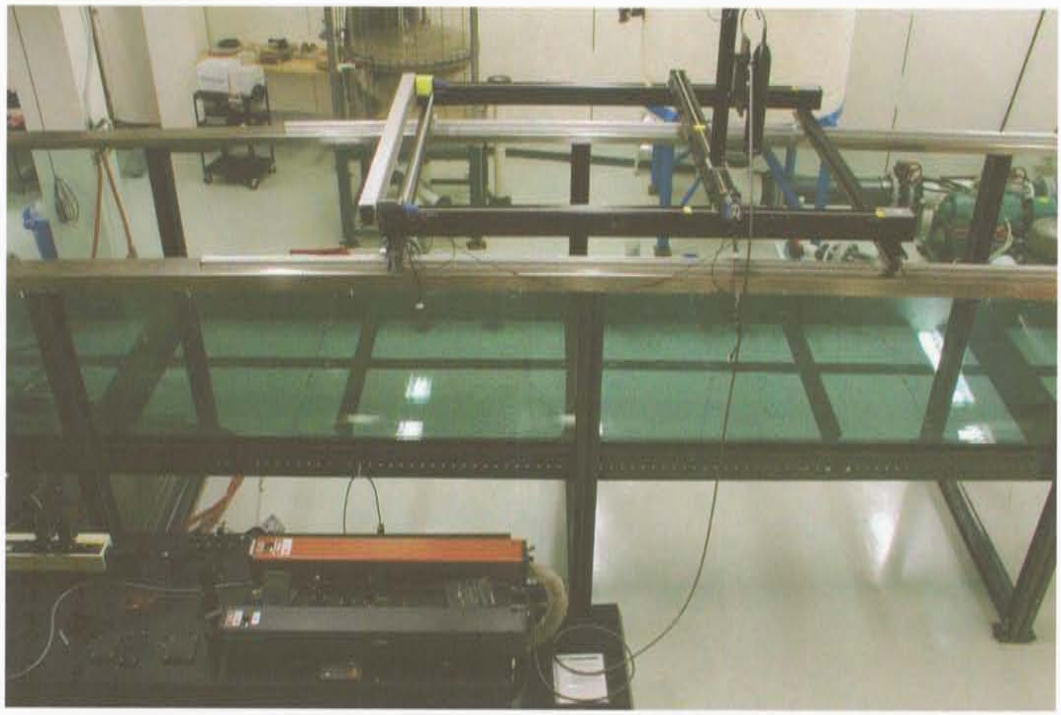

(a)

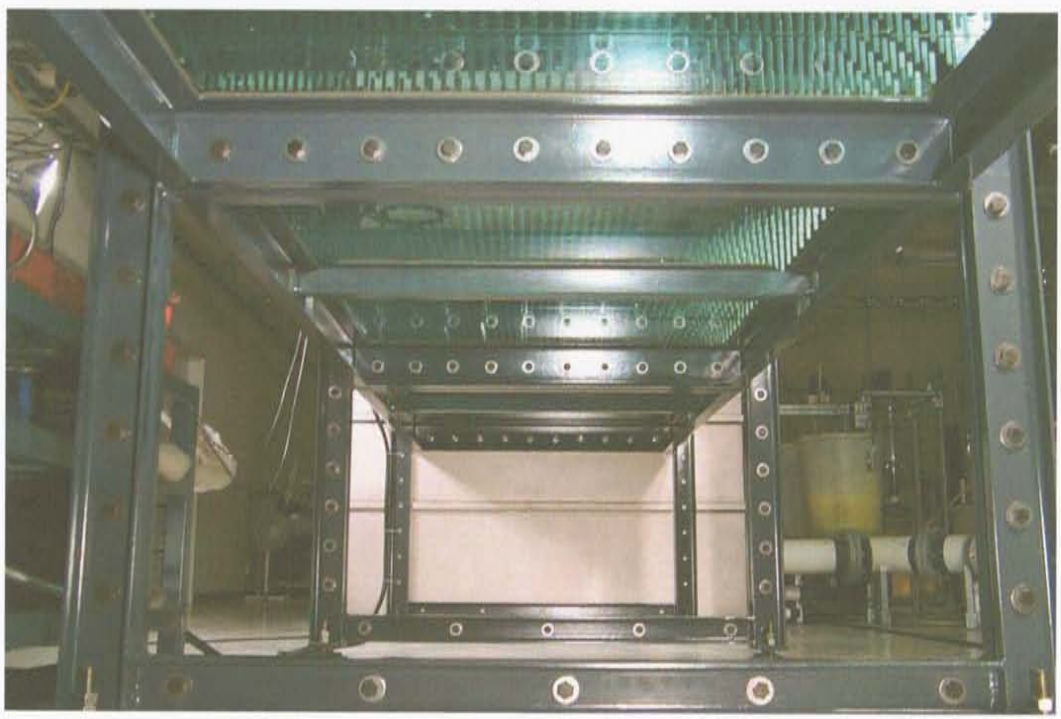

(b)

Figure 2: (a) View from above clearly showing the glass sides and bottom of the water channel. (b) Glass bottom of the water channel as seen from below.

(a)

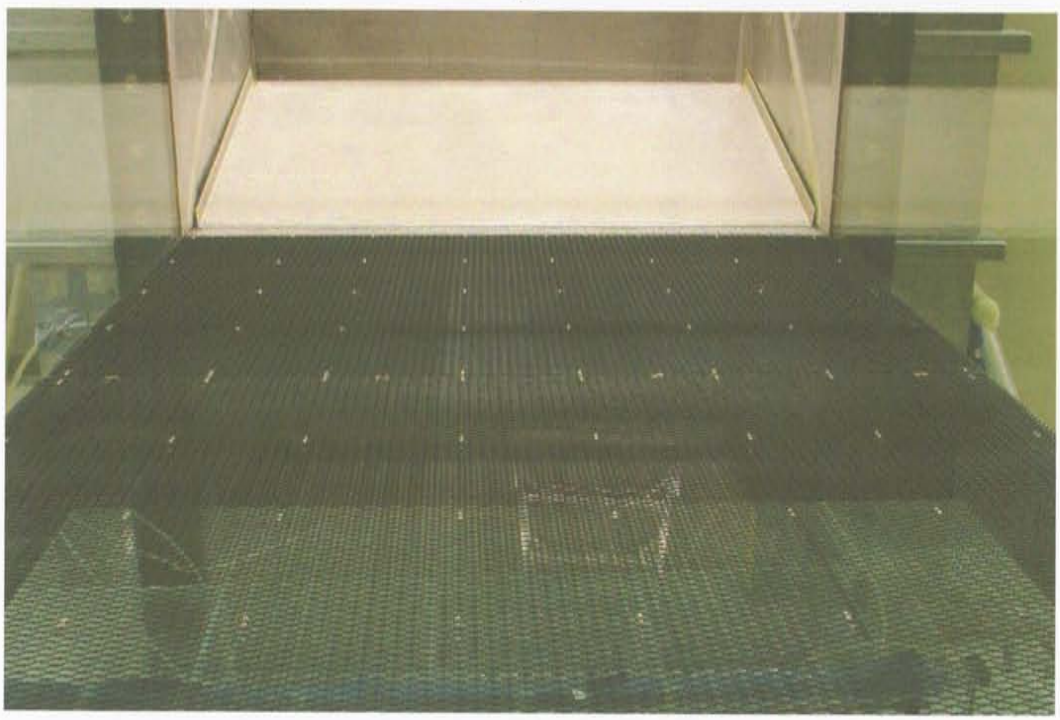

(b)

Figure 3: (a) Inlet plenum with flow conditioning elements. (b) View of outlet plenum showing the adjustable weir gate.

(a)

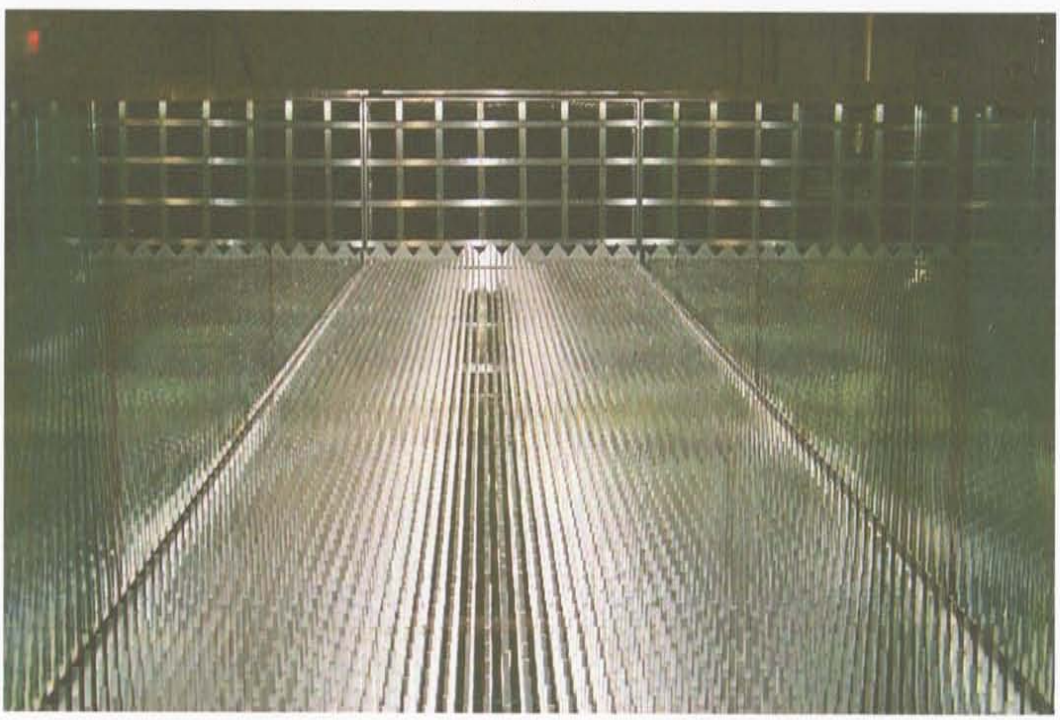

(b)

Figure 4: (a) Inlet flow conditioning elements for the expanded metal surface roughness. (b) Inlet flow conditioning elements for the Raupach array.

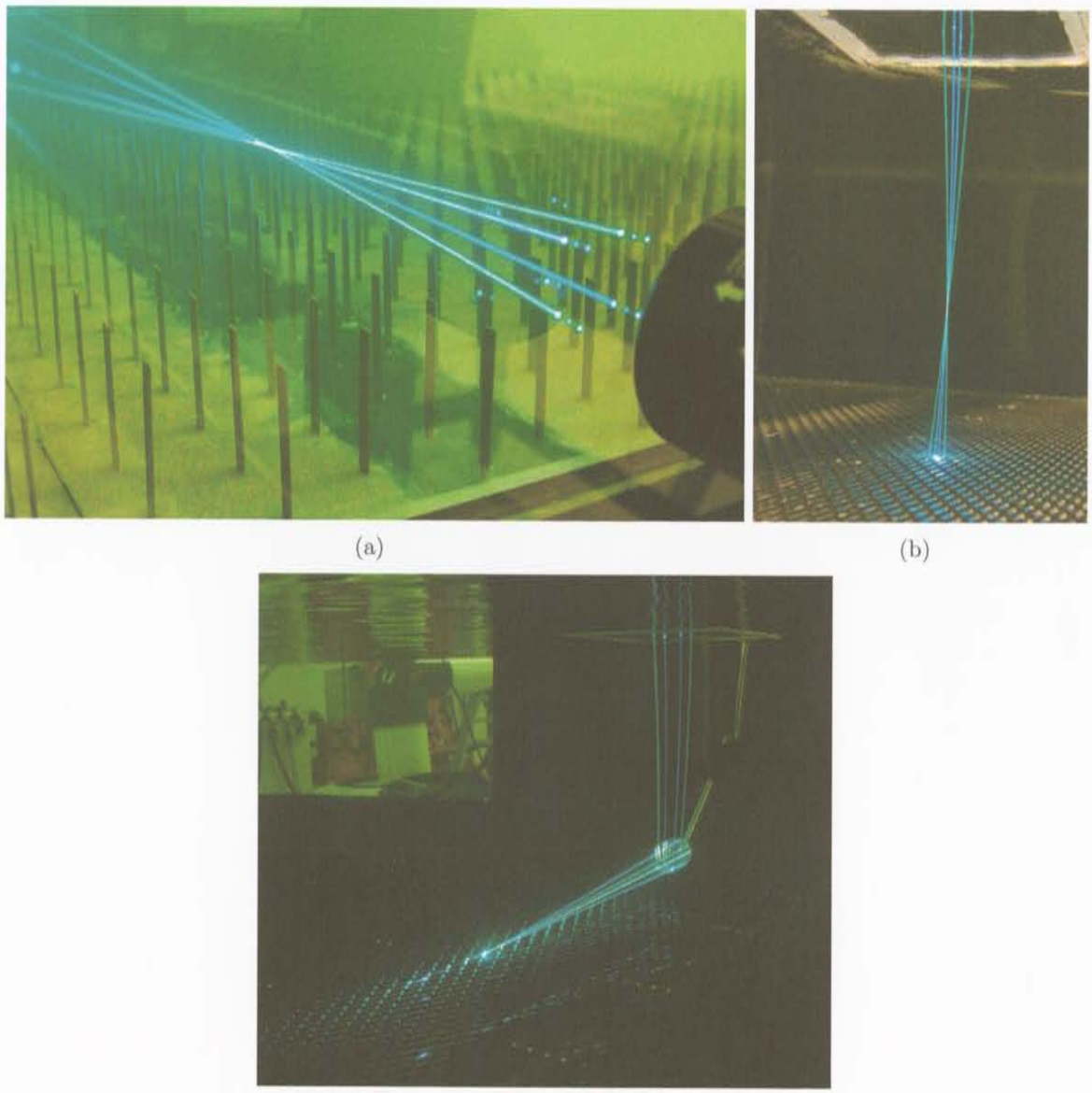

(a) (b)

(c)

Figure 5: (a) LDV probe and beams in the Raupach array configured for measuring uw components. (b) Configuration for measuring uv components from above through a window floating on the surface. (c) Configuration for measuring uw components from above after reflecting off of a mirror.

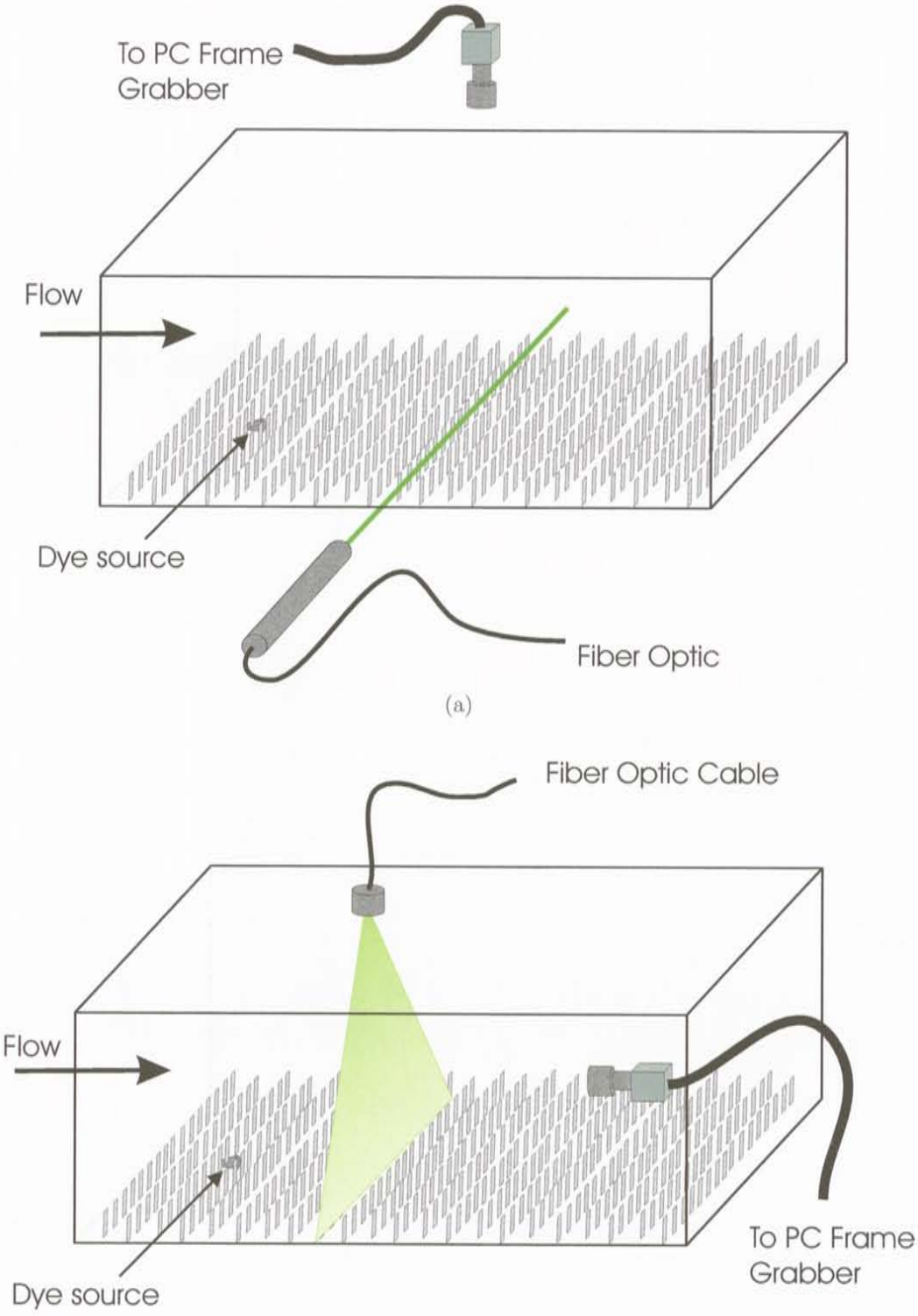

Figure 6: Experimental configurations for LIF concentration measurements (a) 1-D linescan and (b) 2-D area scan.

3 Raupach Array

The first obstacle array configuration tested was the Raupach array. This array was selected to provide a detailed data set that could be compared with the results obtained in a simulated plant canopy array constructed for wind tunnel testing by Raupach et al. (1986); Coppin et al. (1986); Legg et al. (1986). Figure 7 shows the array installed in the water channel.

The vertical stainless steel tabs that make up the array were $H = 60$ mm high, 10 mm wide and 1 mm thick and inserted into laser cut slots in 9.5 mm thick lexan panels. The tabs were arranged in a staggered formation with 60 mm spacing between the centers of the tabs in the cross-stream, y, direction and 44 mm row spacing in the streamwise, x direction. Figure 8 shows the layout of a single unit cell of the array centered on one of the tabs.

The entire test section of the water channel was covered with the roughness array as shown in Figure 7. There were 210 rows of tabs in the channel. Figure 9 is two close-up views of the Raupach array.

The channel was run with the water 0.75 m deep to give an average flow velocity of approximately 0.15 m/s. A saw-tooth fence 14 cm in height and a 36 mm square bar array that can be seen in Figure 7, were placed at the inlet of the water channel, after the contraction from the plenum, to generate some intermediate scale turbulent eddies and speed the development of the boundary layer.

The Raupach array produced aggressive cross-stream and vertical dispersion and required some tuning of the water channel inlet flow conditioning to prevent the development of counter-rotating vortices and cross-stream non-uniformity. After several iterations of LDV testing and modifications to the inlet, the smooth contraction from the plenum into the channel was replaced with a simple straight inlet section extending about 0.85 m into the inlet plenum with the same cross-sectional dimensions (1.5 m wide by 0.9 m deep) as the water channel test section. Two vanes were also added to this extended inlet section to redistribute flow toward the centre of the channel. These two modifications redistributed the flow momentum more uniformly across the channel test section and allowed some boundary layer development prior to the trip fence, square bars, and Raupach array.

3.1 Unit Cell Velocity Data

The Raupach array had a repetitive pattern that can be described by defining a unit cell centered on a tab as shown in Figure 8. Detailed velocity measurements were obtained in a unit cell centered on the 7th tab ($y = 420$ mm from the sidewall) of row 160 ($x = 7040$ mm downstream). The measurements were made off-centre in the channel to take advantage of the better quality data produced by shorter focal length LDV lenses.

The velocity measurements included both uw and uv components measured at 19 different positions, labelled A through S, in the unit cell illustrated in Figure 8. Points A through J were based on the original Raupach et al. (1986) measurements. Points K through S were added to provide some additional detail.

LDV measurements require a clear optical path through the tab array so it was necessary to shift some of the points from the ideal coordinates as shown Figure 8 to get around the tabs that were obstructing the beams. For example, there were no uw measurements

below $z = 0.3$H because the incoming beams were cut off by the channel bottom. The uv components were measured down to $z = 0.1$H but there were no measurements of the uv components at positions A and R because the tab interfered with the incoming beams.

The Raupach average velocity calculated in the spreadsheets and shown on some of the plots was taken from Raupach et al. (1986):

$$\text{Raupach average velocity} = \frac{\text{Velocity at point}(A + B + 2C + D + E + \left(\frac{F+G}{2}\right) + 2H + 2I + J)}{12} \quad (1)$$

Some samples of the velocity statistics available are shown in Figures 10 to 12.

3.2 1-D Linescan LIF Concentration Data

The dye source illustrated in Figure 13 was placed immediately behind the centre ($y = 0$) tab in row 116 of the array ($x = 5104$ mm). The centre of the 15 mm diameter source was at $z = 0.2H = 12$ mm above ground level. The front of the source was 26 mm downstream of row 116 and dye was emitted in the downstream direction at a flow rate of 24 ml/min. The source was designed to emit the dye with minimal momentum and to be relatively large to eliminate directional sensitivity. A very small source tended to be sensitive to the exact placement in the array and could be biased to one side or the other of the channel by very small changes in the position or angle of the release.

All of the measurements of concentration were made halfway between rows of tabs and are referenced to the source position. For example, the source was at row 116 and the front of the source was approximately halfway between rows 116 and 117. The first set of measurements was made at 1 row downstream of the source halfway between row 117 and 118. This position was 40 mm downstream of the source (the row spacing was 44 mm, and the source was 26 mm from row 116 so the distance from the source to halfway between row 116 and 117 was only 40 mm). The measurements at 2 rows downstream were made halfway between rows 118 and 119 at 40+44 = 84 mm from the source. At 8 rows downstream, halfway between rows 124 and 125, the measurement position was $40 + 7 \times 44 = 348$ mm from the source. Concentration data coordinates are given in the plots and spreadsheets in positions relative to the source x and y location and ground level $z = 0$.

Two types of linescan measurements were made. Horizontal line measurements were made with the configuration shown in Figure 6 at 1, 2, 4, 7, 8, 12, and 16 rows downstream of the source at approximately 8 z positions. Vertical linescan measurements were made along the centerline of the source (i.e. $y = 0$) by interchanging the linescan camera and laser beam positions.

All Raupach linescan measurements were collected for total sample times of 2000 seconds at sampling rates of 300 Hz for a total of 600,000 samples per pixel. The sources were turned on before the data collection began and turned off after the data collection stopped so that all releases were continuous releases without startup or end effects.

Sample plots of the basic statistical values are contained in Figures 14 and 15. The concentration statistics values are described in Appendix C.

3.3 2-D Area Scan LIF Videos

The 2-D full field images are most useful for examining the overall structure of the plume. A laser sheet was shone vertically into the channel along a $y - z$ plane through the plume as shown in Figure 6(b). On the data CD's there are seven AVI files that contain 2 minute real-time movies of the plume cross-section at various downstream positions. All of the images are false colored to improve the contrast between different concentration levels. Black is zero concentration, white is the maximum measurable concentration and the range from blue to green to red covers the low to high concentrations. Figure 16 shows a sample instantaneous plume snapshot and the average concentration distribution computed by averaging all of the frames in the `*.avi` file.

As previously discussed, these 2-D images are best used for qualitatively examining plume structure. The images were calibrated and corrected for background levels and light sheet non-uniformity, but suffer in quality from the relatively small dynamic range of the analog 8-bit digitized camera.

(a)

(b)

Figure 7: (a) Overall view of Coanda's water channel with the Raupach array installed. (b) View of the Raupach array looking upstream inside the water channel.

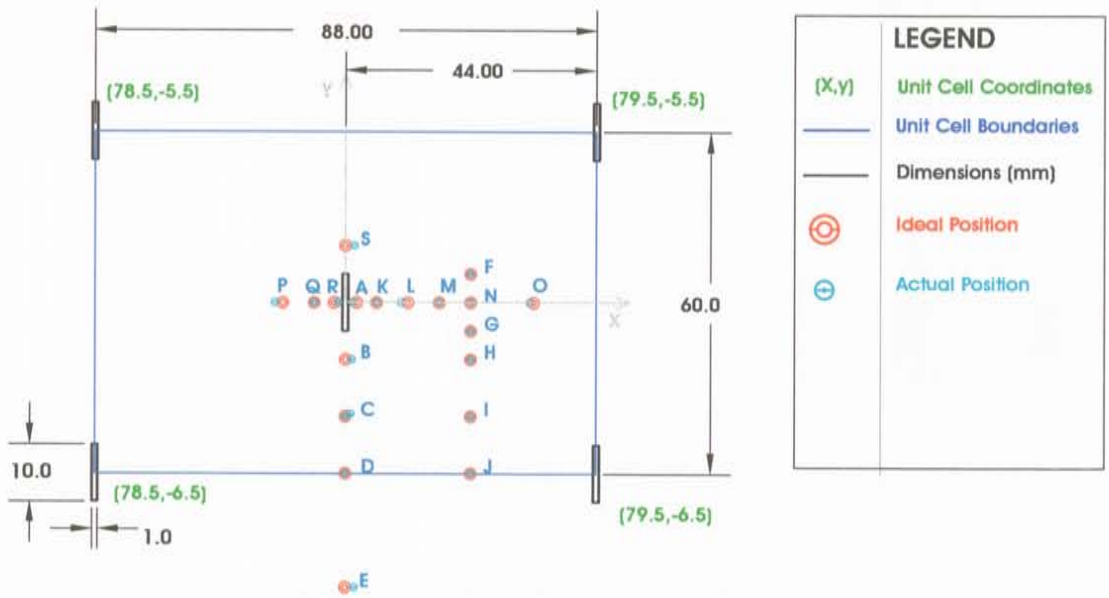

Figure 8: Schematic of the Raupach unit cell.

(a)

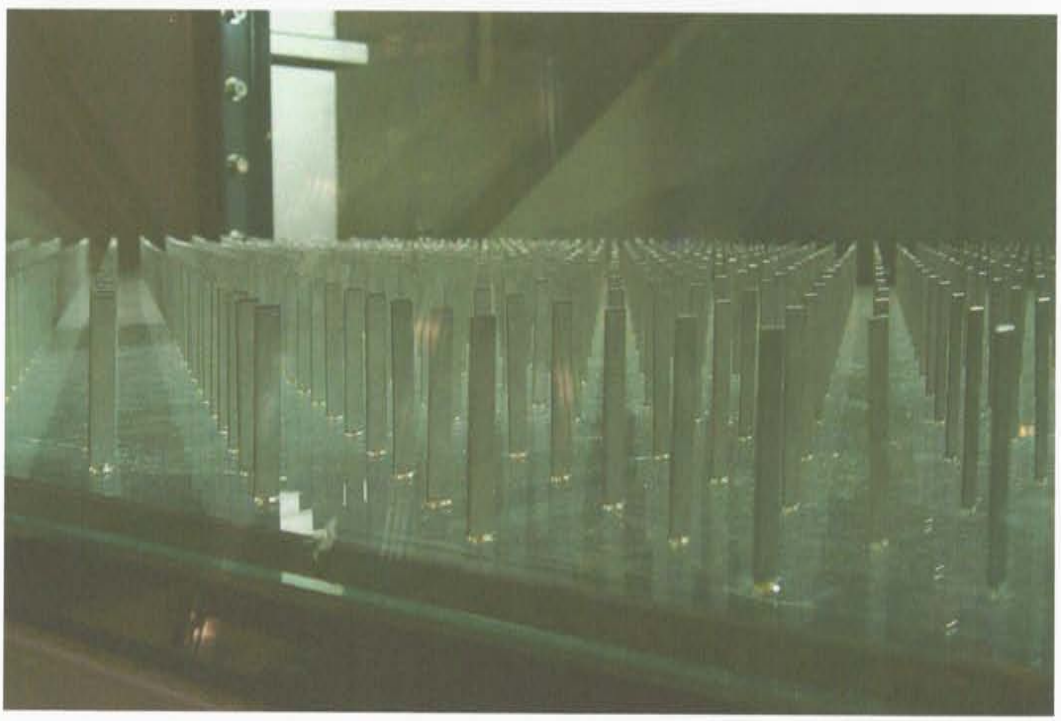

(b)

Figure 9: Two close-up views of the Raupach array showing the staggered arrangement of stainless steel tabs.

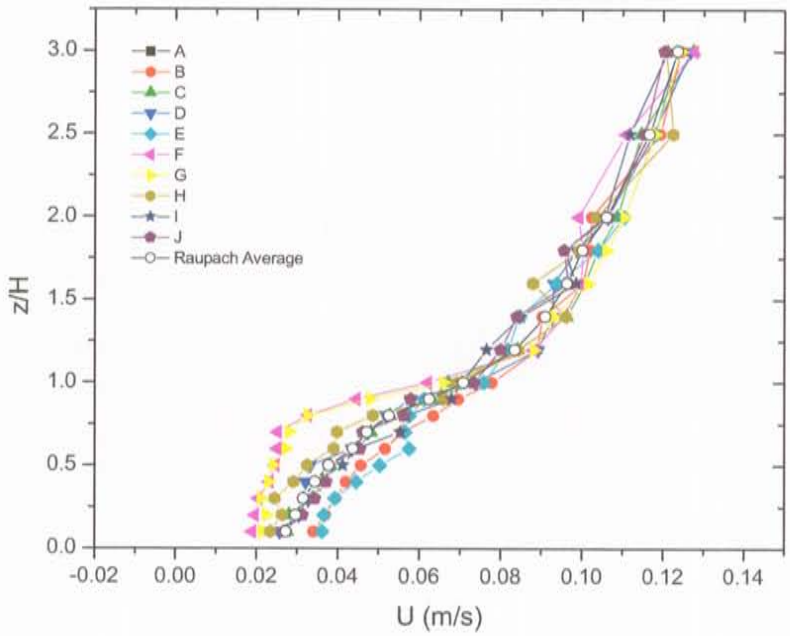

(a)

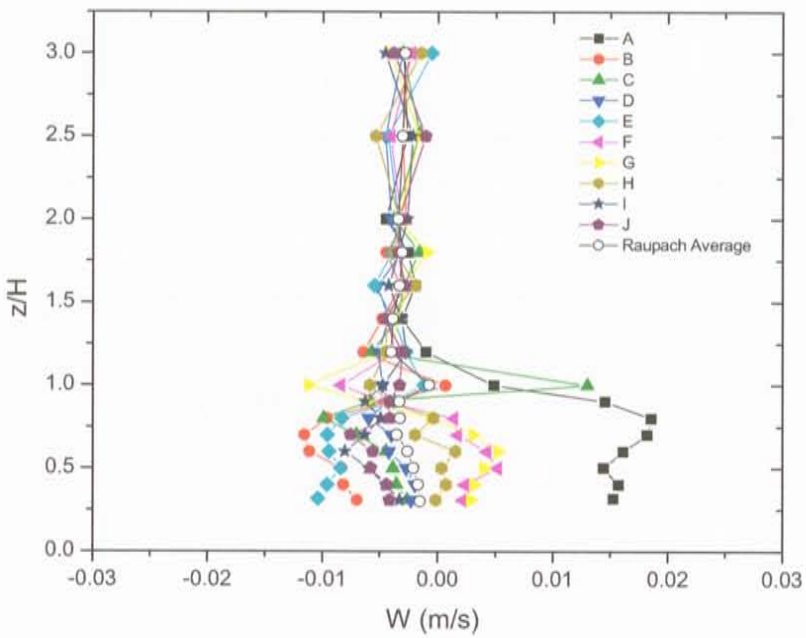

(b)

Figure 10: Unit cell velocity profiles at the 12 Raupach positions A through J. (a) mean streamwise velocity U. (b) mean vertical velocity W.

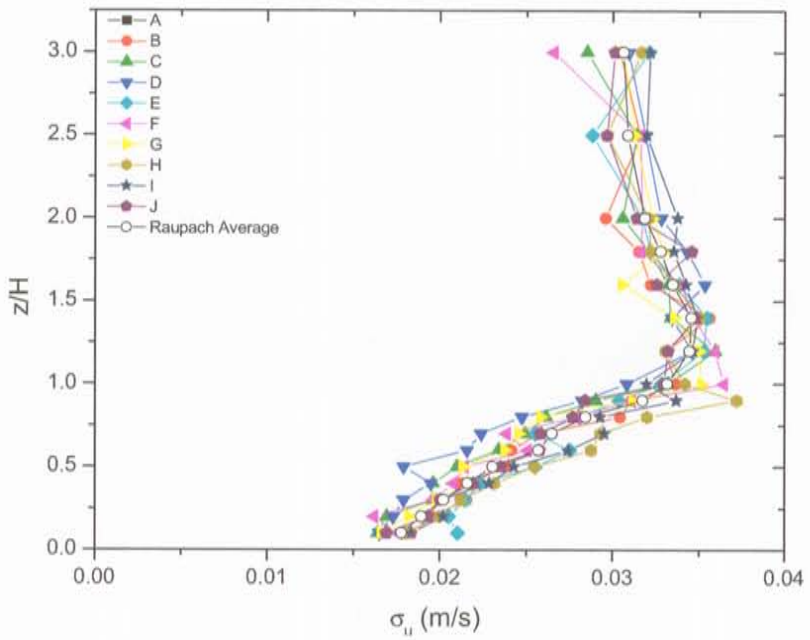

(a)

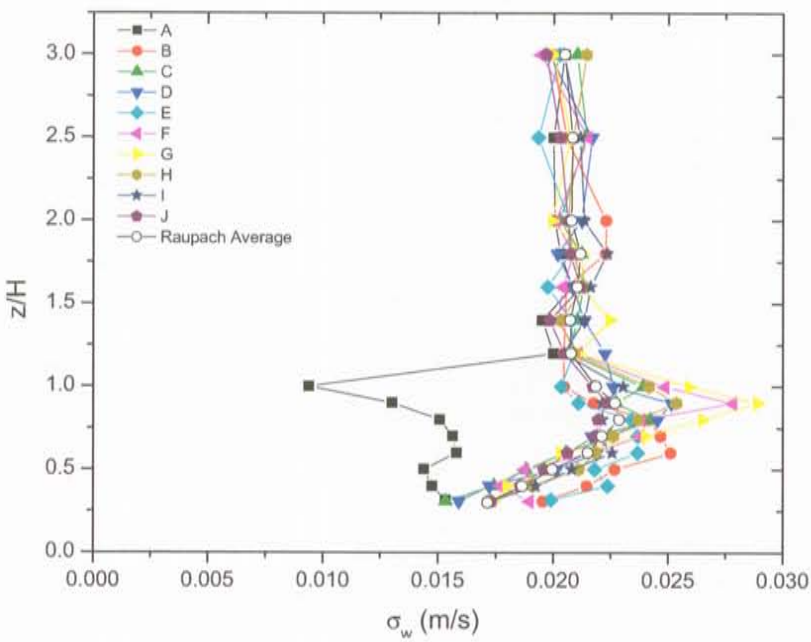

(b)

Figure 11: Unit cell velocity profiles at the 12 Raupach positions A through J. (a) streamwise velocity standard deviation σ_u. (b) vertical velocity standard deviation σ_w.

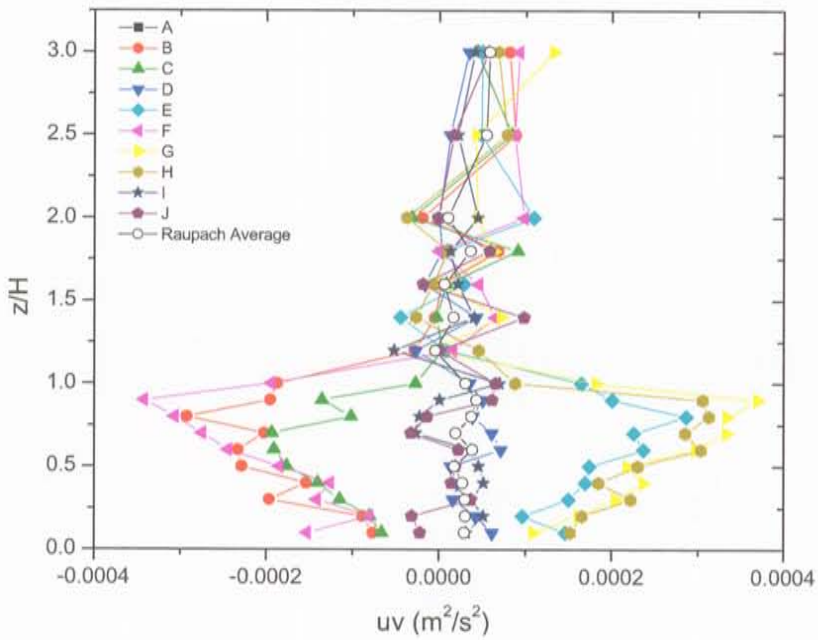

(a)

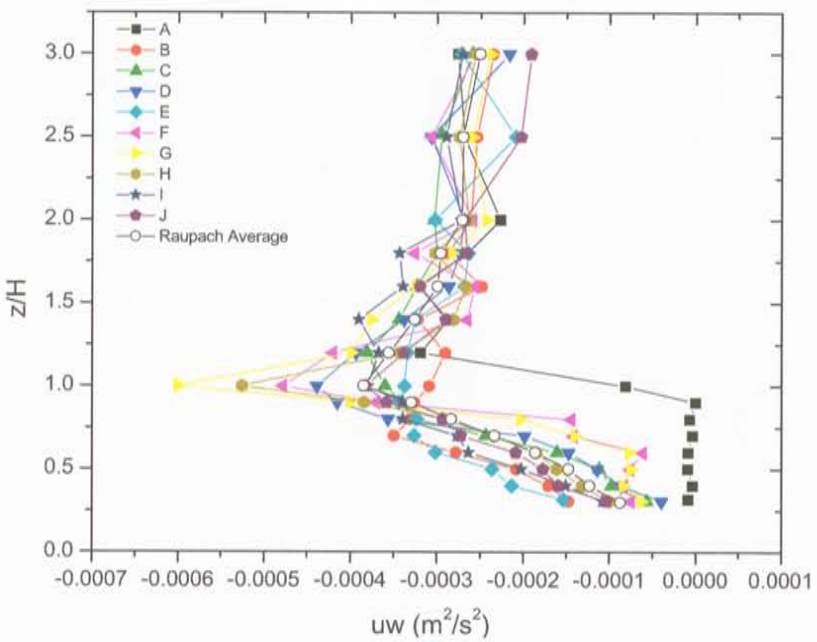

(b)

Figure 12: Unit cell velocity profiles of Reynolds stress at the 12 Raupach positions A through J. (a) $\overline{u'v'}$ (b) $\overline{u'w'}$

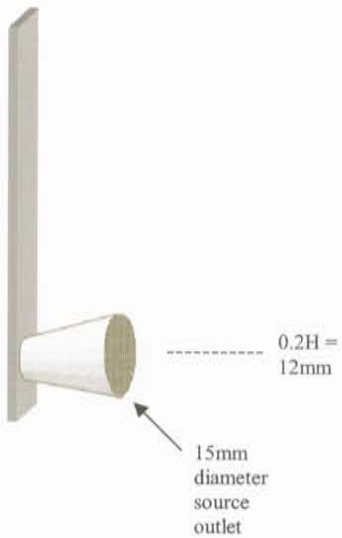

Figure 13: Fluorescein dye source attached to the downstream side of a Raupach tab. There was a fine mesh screen covering the source outlet to ensure even distribution across the entire outlet area. The centreline of the source was at $z = 0.2H = 12$ mm above the ground.

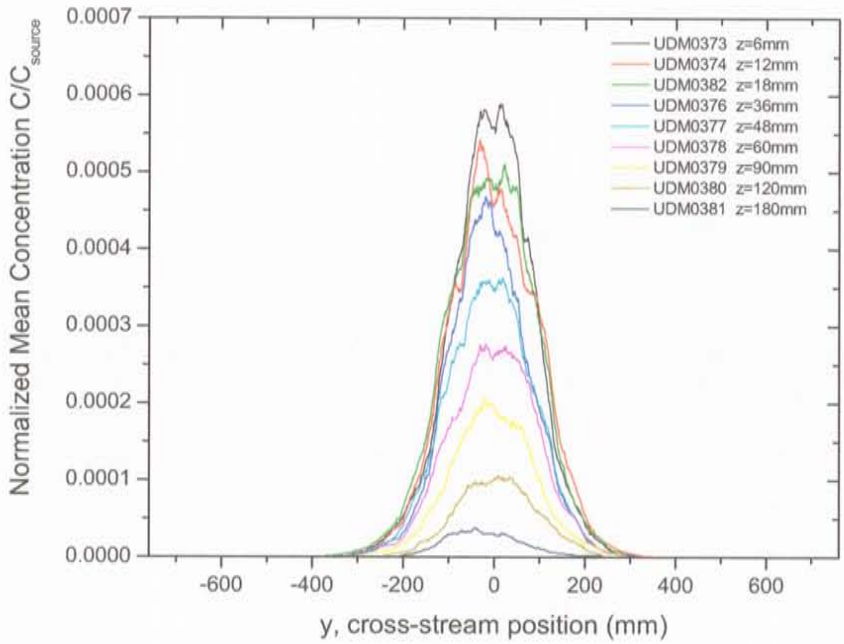

(a)

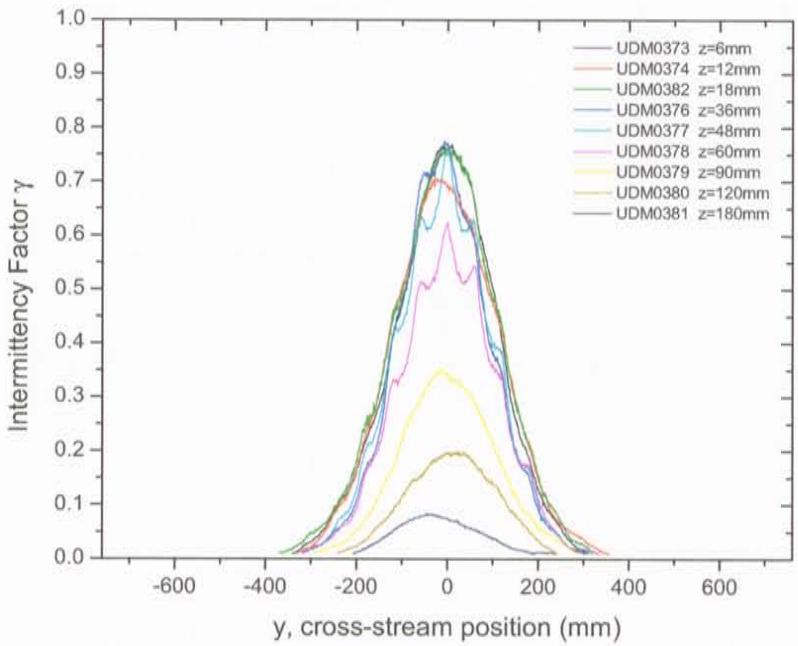

(b)

Figure 14: Concentration statistics at 4 rows (172 mm) downstream of the source in the Raupach array. (a) mean concentration C (b) intermittency factor γ

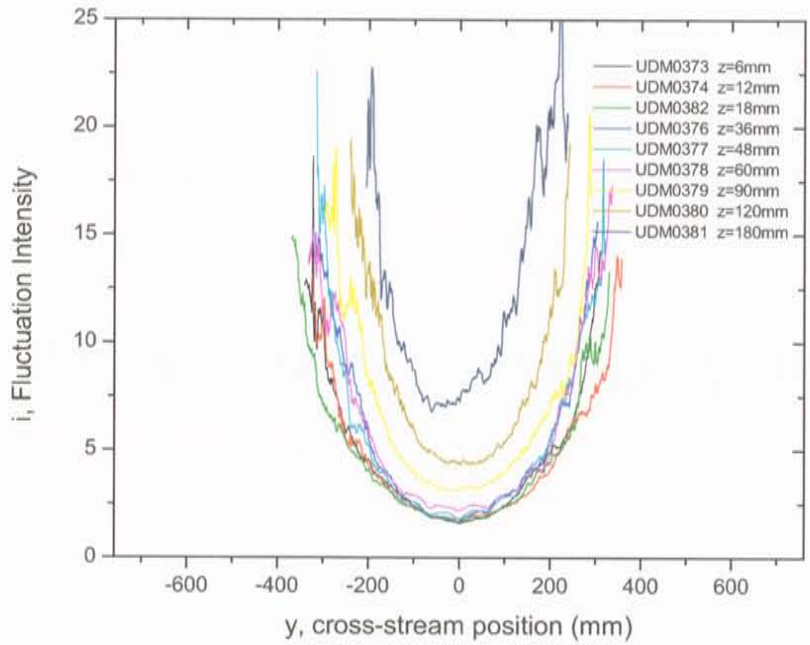

(a)

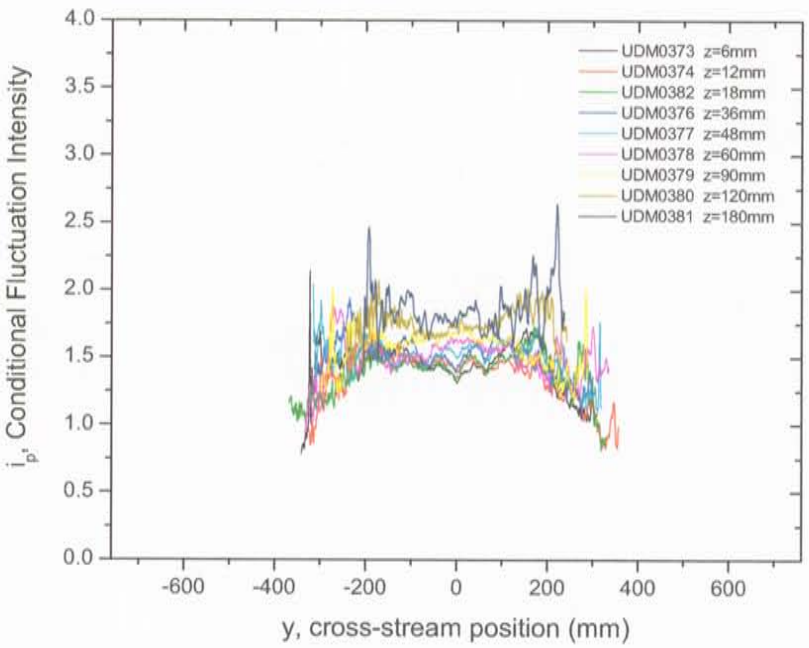

(b)

Figure 15: Concentration statistics at 4 rows (172 mm) downstream of the source in the Raupach array. (a) fluctuation intensity i (b) conditional fluctuation intensity i_p

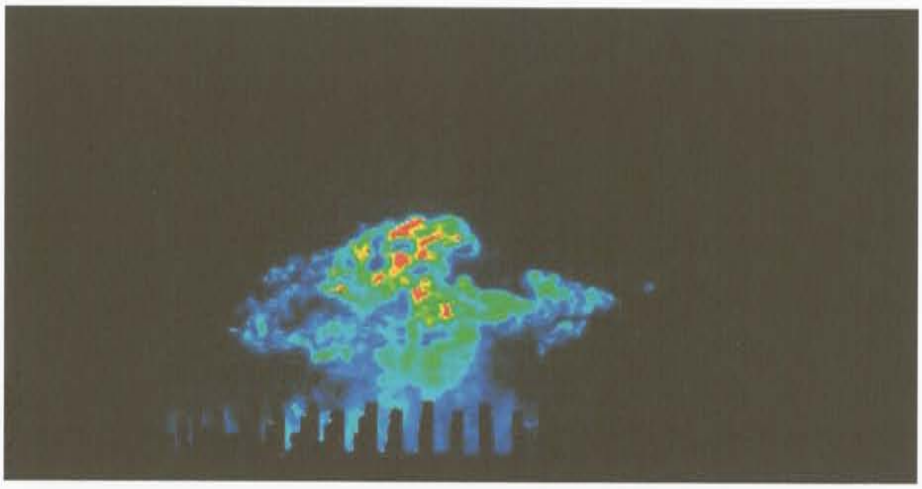

(a)

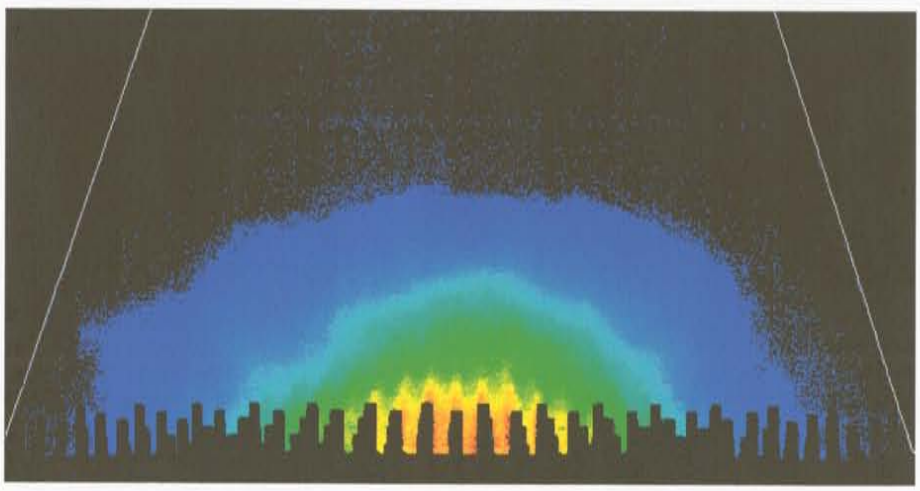

(b)

Figure 16: Sample 2-D concentration profiles on a $y - z$ plane 8 rows downstream of the source in the Raupach array. (a) instantaneous plume cross-section (b) average concentration profile.

4 MUST Array

The Mock Urban Setting Test (MUST) array was tested as part of a larger project by the Technical Cooperation Programme (TTCP) Chemical and Biological Defence (CBD) Group, Technical Panel 9 (TP-9). Several countries cooperated to compare the results obtained from measurements in the same urban obstacle array at different scales in different experimental configurations. The full scale case was tested in the fall of 2001 at the Dugway Proving Grounds in Utah with an array of shipping containers as shown in Figure 17 and reported in Biltoft (2001). Wind tunnel tests were done at Monash University in Australia at approximately 1:50 scale. Water channel tests were performed by Coanda at 1:205 scale.

The full scale dimensions of the MUST obstacles were 12.18 m long, by 2.42 m wide by 2.54 m high. In the full scale tests, the rows of obstacles were spaced 12.9 m apart on average and the columns were spaced 7.9 m apart on average (rows were perpendicular to the expected flow direction and columns were parallel to the flow). The water channel experiments were scaled down to 1:205 so the laboratory obstacles were 59.4 mm long by 11.8 mm wide by $H = 12.4$ mm high with rows spaced 62.9 mm apart and columns spaced 38.5 mm apart. Figure 18 is a drawing of the 1:205 scale obstacles and Figure 19 shows the layout of the array with the source position and the velocity measurements positions. Figure 20 shows the anodized aluminum MUST obstacles installed on the lexan panel.

The water channel was reconfigured to accommodate the MUST experiment. Water depth was reduced to 0.3 m to raise the average flow velocity and produce a sufficiently high Reynolds number based on the very short obstacle height of 12.4 mm. In addition, a surface roughness of black anodized 1/2 x 18 gauge raised surface expanded metal was installed in the bottom of the water channel and around the obstacle array to produce the required rough-surface turbulent boundary layer. The expanded metal had diamond shaped holes that were approximately 11 mm across in the streamwise x direction and about 25 mm wide in the cross-stream y direction. The total thickness of the expanded metal was about 4 mm. Figure 21 is a picture of the surface roughness installed in the channel and a close-up of the expanded metal.

4.1 MUST - Velocity Measurements

Velocity measurements of the uv and uw components were made at several locations within the 10x12 MUST obstacle array as shown in the drawing in Figure 19. The reference position for MUST velocity positions was the centre of the array. Sampling time was 500 seconds at all positions.

Vertical profiles were measured through the array at points in the canyon between columns of obstacles (points A through H) as well as directly behind obstacles (points I through P). Some additional measurements (points AA through LL) were made closer to an obstacle near the centre of the array. Measurements were also made without the MUST obstacles and only the surface roughness in position. These no-obstacle tests provided a basis for evaluating the differences between the flow field with and without obstacles. Figures 22 to 24 are samples of the velocity measurements.

4.2 MUST - 1D Linescan LIF

The dye source for all of the MUST concentration measurements was a small diameter vertical jet source made from a 3.1 mm outer diameter, 2.8 mm inner diameter stainless steel tube. The tube was installed so it emitted dye vertically with the top of the source at the same level as the top of the expanded metal roughness (i.e. at $z = 4$ mm) as shown in Figure 25. The source was placed halfway between rows 1 and 2 near the fifth obstacle from the side of the channel at positions L or D, as shown in Figure 19. The source flow rate was 12 ml/min. At this low source velocity, the released material was entirely caught in the wake of the upstream obstacle before it dispersed downstream. Qualitative observations of other types of sources showed that there was little difference between source types as long as the momentum of the source was low.

Linescan 1D LIF measurements were made in several different configurations at several downstream positions. Sample time for each measurement position was 1000 seconds:

MUST001 - source behind the 5th column obstacle between rows 1 and 2, position L in Figure 19. Sample plots of the linescan statistics from MUST001 are shown in Figures 26 to 27

MUST002 - source in the canyon between obstacle columns and rows 1 and 2, position D in Figure 19.

MUST003 - same expanded metal roughness as the MUST array, but no obstacles.

MUST004 - same configuration as MUST001, but without the expanded metal roughness around the obstacles.

MUST005 - same configuration as MUST001, but with no expanded metal roughness upstream or around the obstacles.

MUST006 - no roughness or obstacles just flat lexan panels on the bottom of the entire length of the channel.

4.2.1 MUST - 1D Linescan LIF Puff Measurements

In addition to the continuous sources in MUST tests 001 to 006, some tests were made with short duration puff releases. The release sequence for each puff was triggered at time $t = 0$. At time $t = 3$ seconds the 0.5 ml puff of fluorescein dye was released at a rate of 24 ml/min producing a puff duration of 1.25 seconds ending at time $t = 4.25$ seconds. Data were collected for duration of 10,000 line samples at 300Hz up to $t = 33.33$ seconds. There was some uncertainty in the puff start time on the order of ± 0.5 seconds caused by variability in the pump triggering and in the process used to separate individual puffs from a single data file containing many puffs. Series of 100 puffs were released for each measurement position. Measurements were made both with and without obstacles. Figures 28 to 29 show some sample statistics calculated from the ensemble of 100 puffs.

MUST007 - same array configuration as MUST001, but releases were series of 100 short puffs of dye rather than continuous releases.

MUST008 - same array configuration as MUST003, roughness but not obstacles, 100 short puff releases.

4.3 MUST - 2D LIF

Full field 2D images in the $y-z$ plane were taken at four downstream positions in the MUST array. The AVI files can be found on the data CD's. As with the Raupach array, these real-time movies are most useful for qualitative evaluation of plume structure. All of the images are false colored to improve the contrast between different concentration levels. Black is zero concentration, white is the maximum measurable concentration and the range from blue to green to red covers the low to high concentrations. Figure 30 shows a sample instantaneous plume snapshot and the average concentration distribution computed by averaging all of the frames in the `*.avi` file.

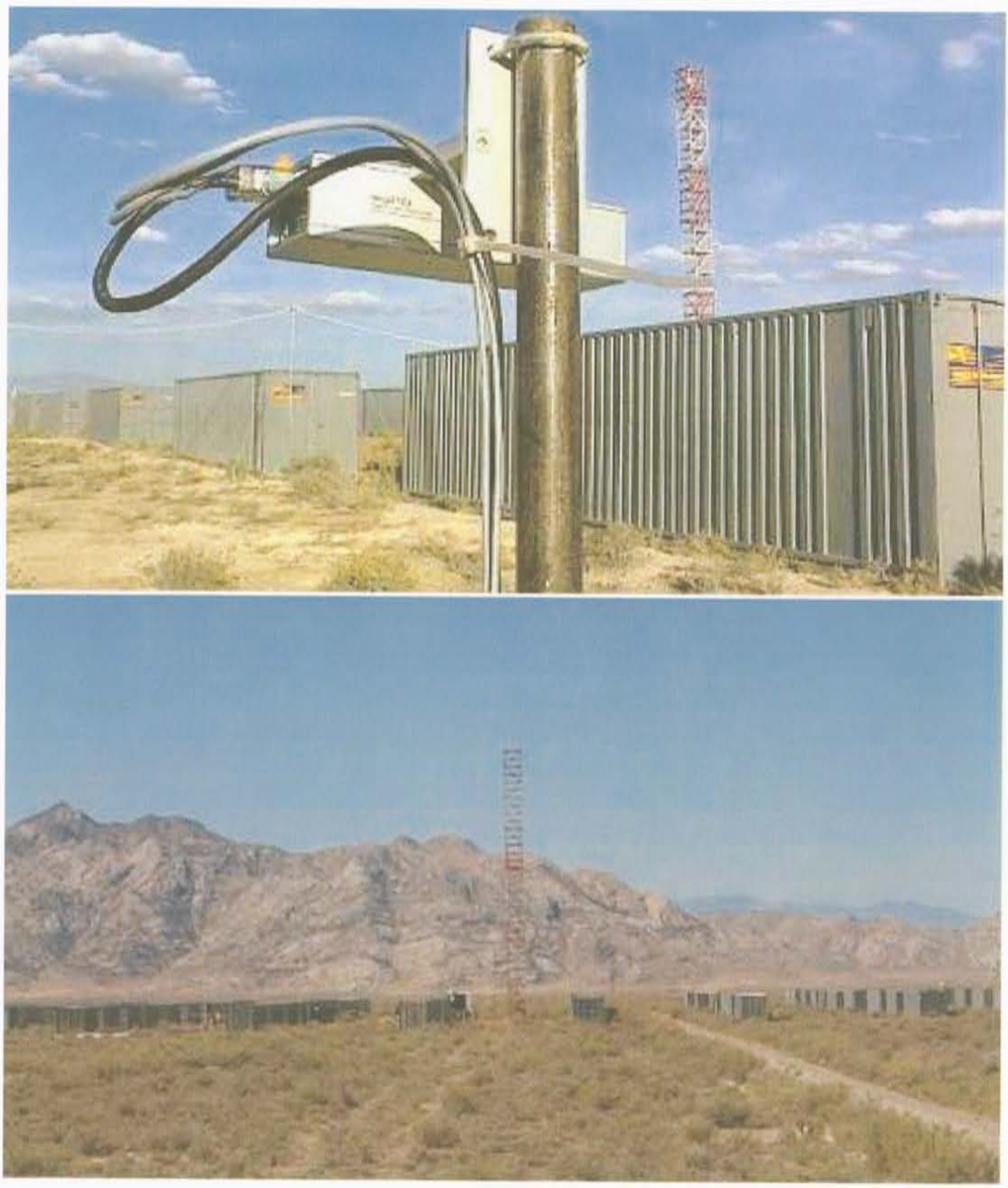

Figure 17: Photographs of the full-scale MUST tests at Dugway Proving Grounds in Utah.

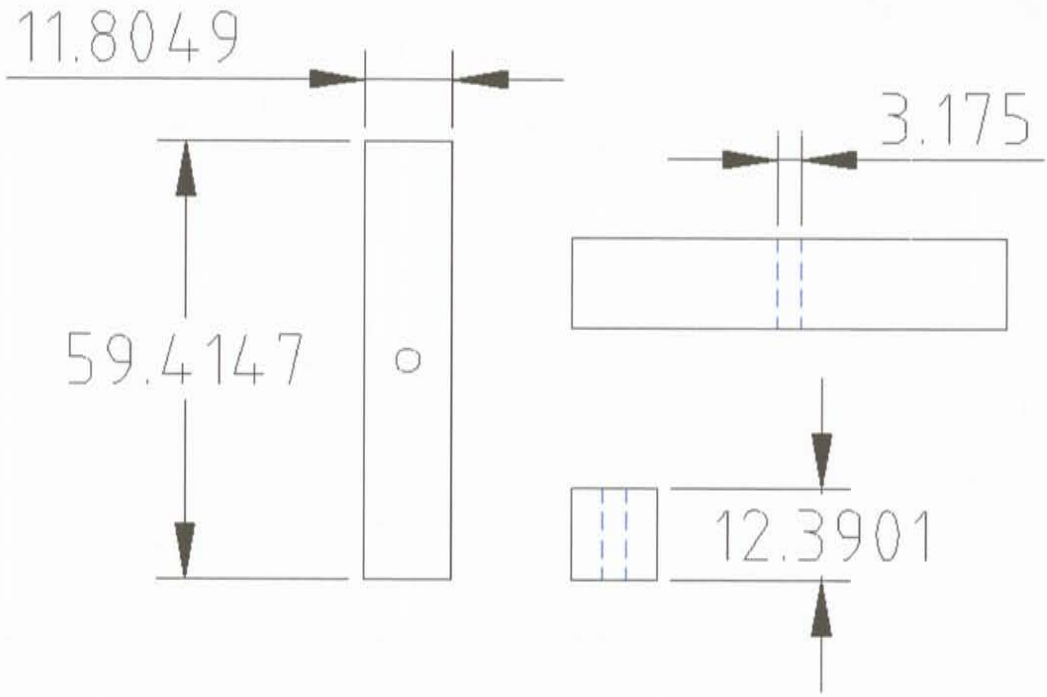

Figure 18: Water channel 1:205 scale MUST obstacle dimensions (mm).

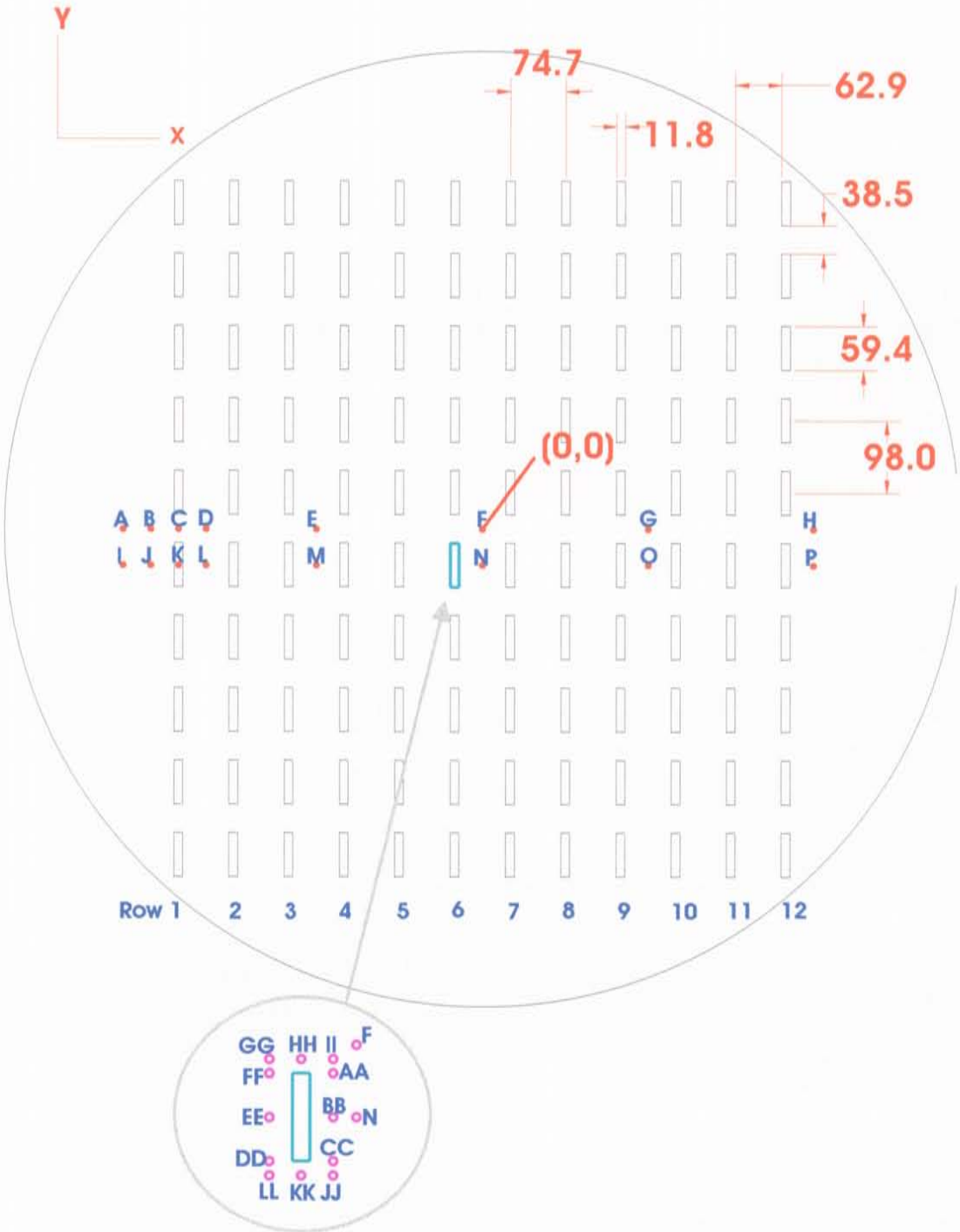

Figure 19: MUST array layout with velocity measurement positions. The reference point is the centre of the array at (0,0). The small inset picture shows the position of velocity measurement points around a single obstacle near the centre of the array.

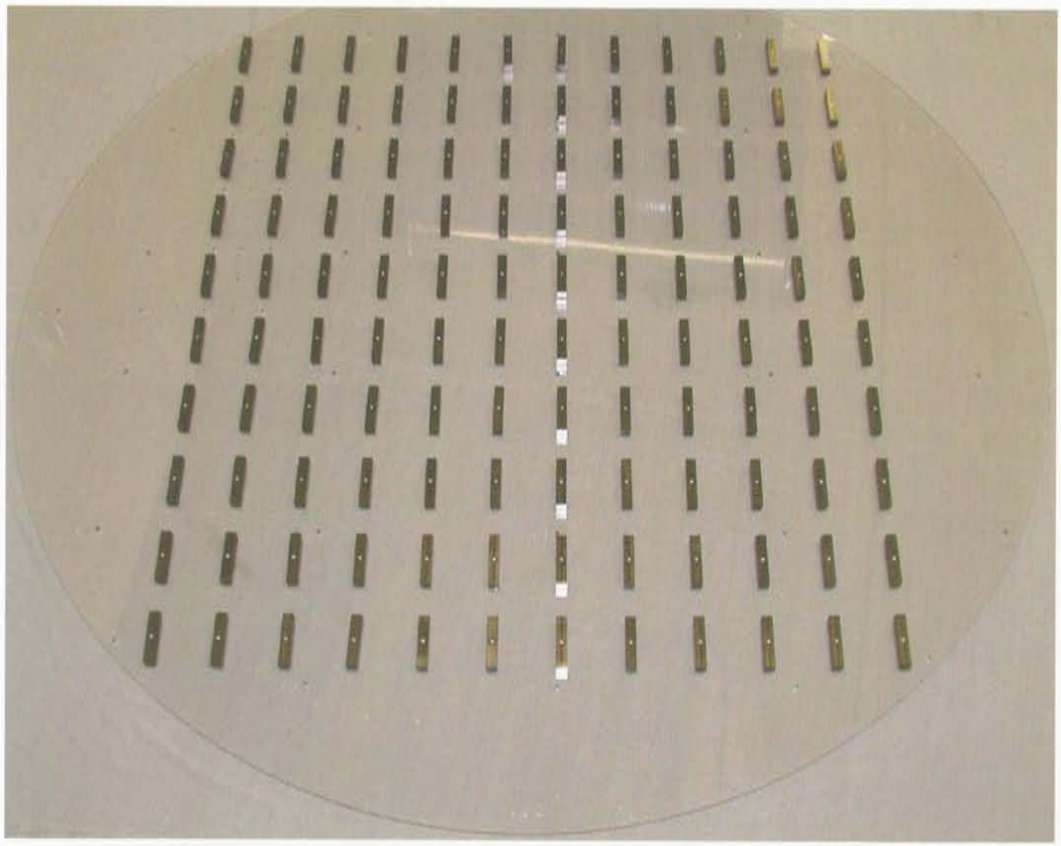

(a)

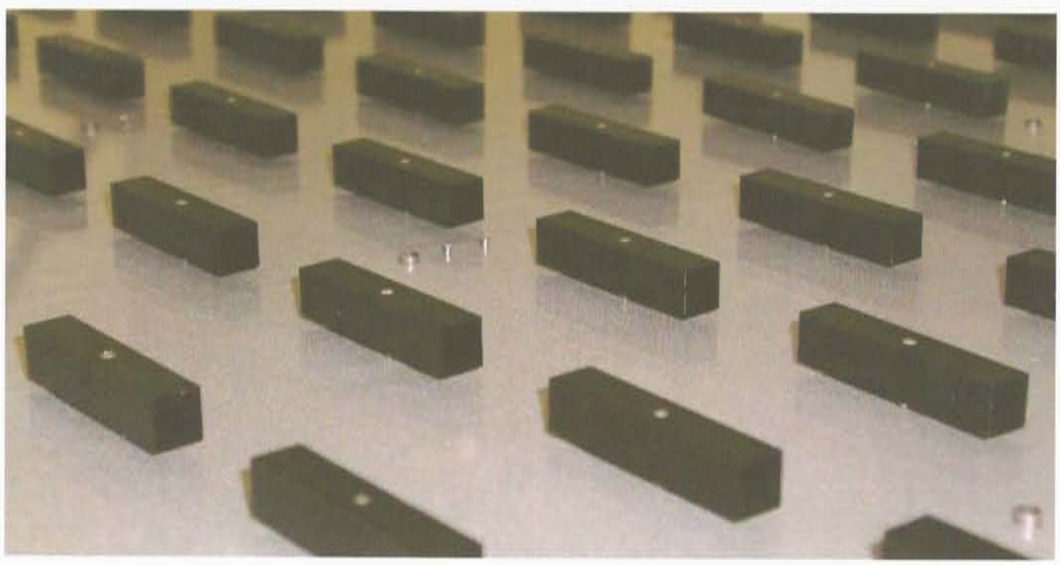

(b)

Figure 20: (a) MUST array on the turntable. (b) Close-up of the MUST obstacle array.

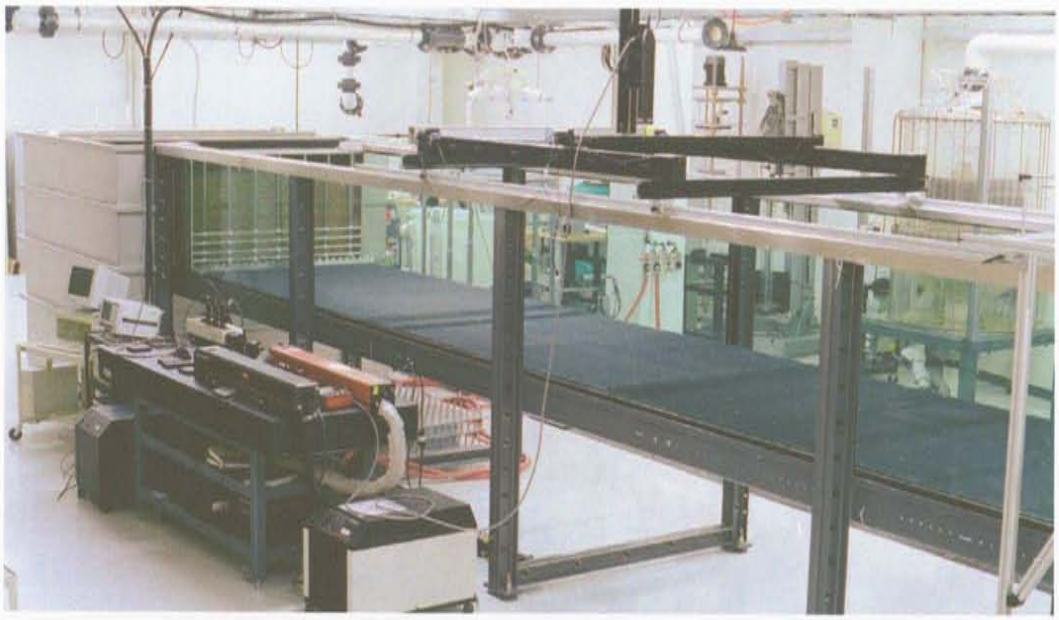

(a)

(b)

Figure 21: (a) Expanded metal roughness installed in the water channel. (b) Close-up of the expanded metal surface roughness.

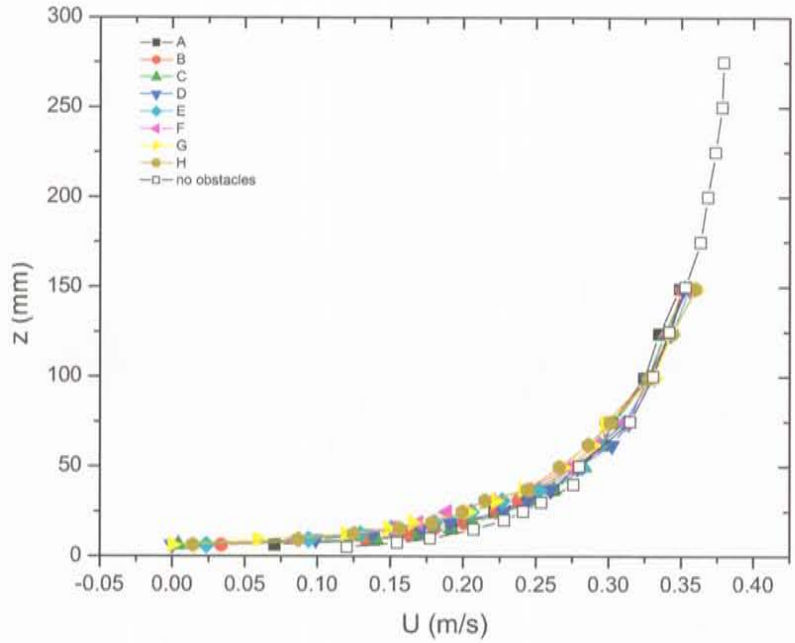

(a)

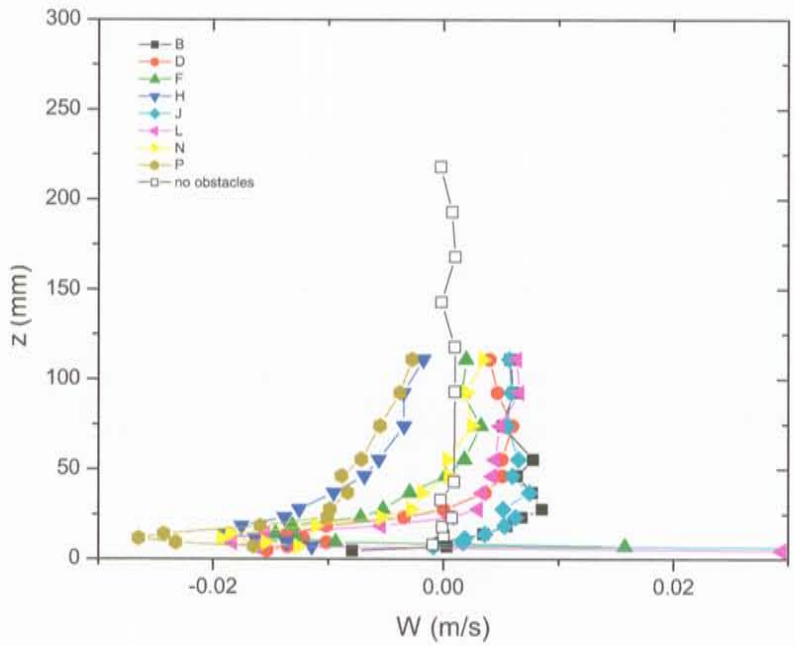

(b)

Figure 22: MUST array velocity profiles at points A through H on the array cross-stream centreline (a) streamwise mean velocity U (b) vertical mean velocity W.

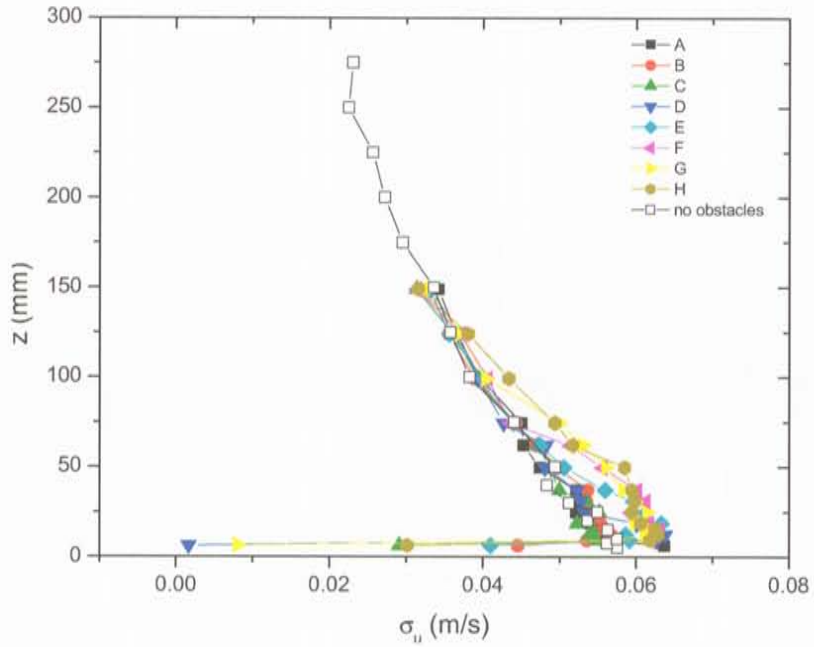

(a)

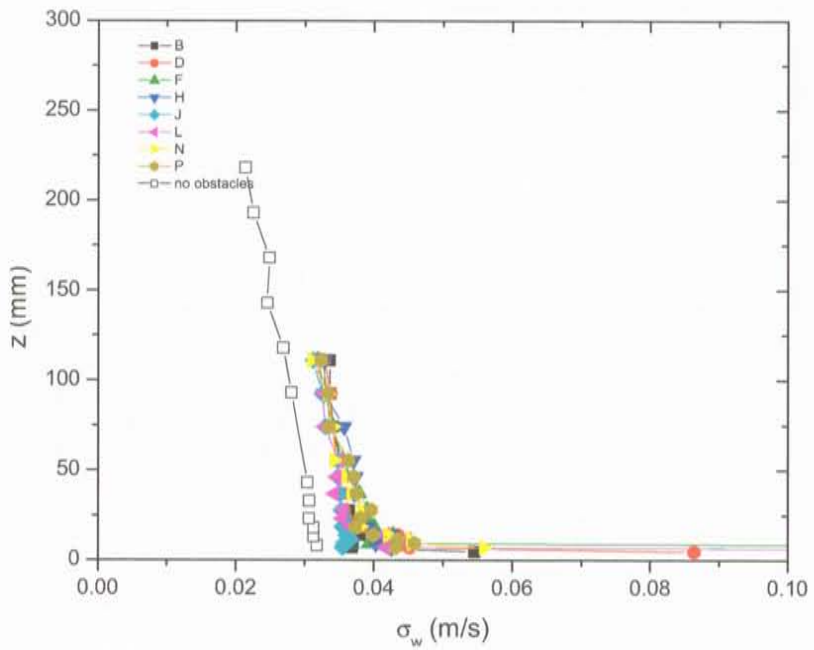

(b)

Figure 23: MUST array velocity standard deviations at points A through H on the cross-stream array centreline (a) streamwise velocity component σ_u (b) vertical velocity component σ_w.

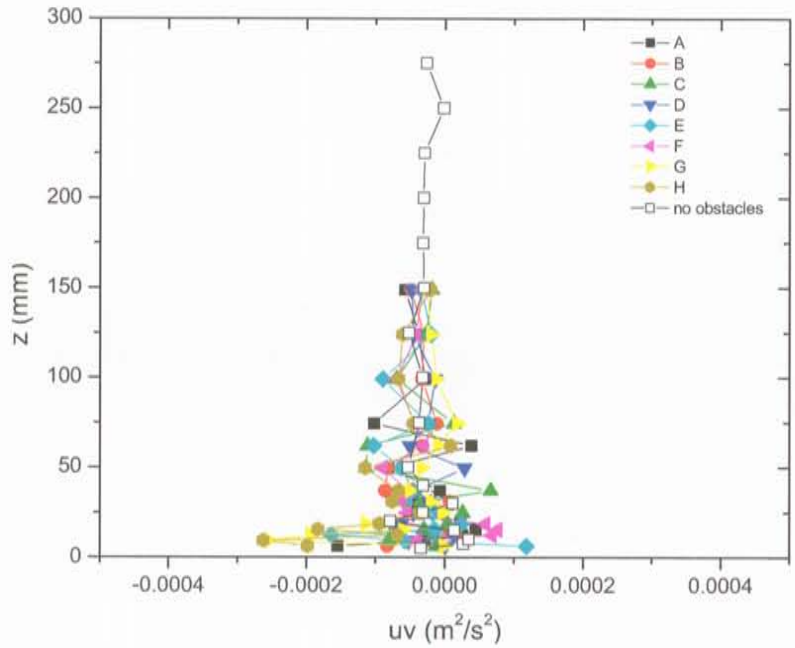

(a)

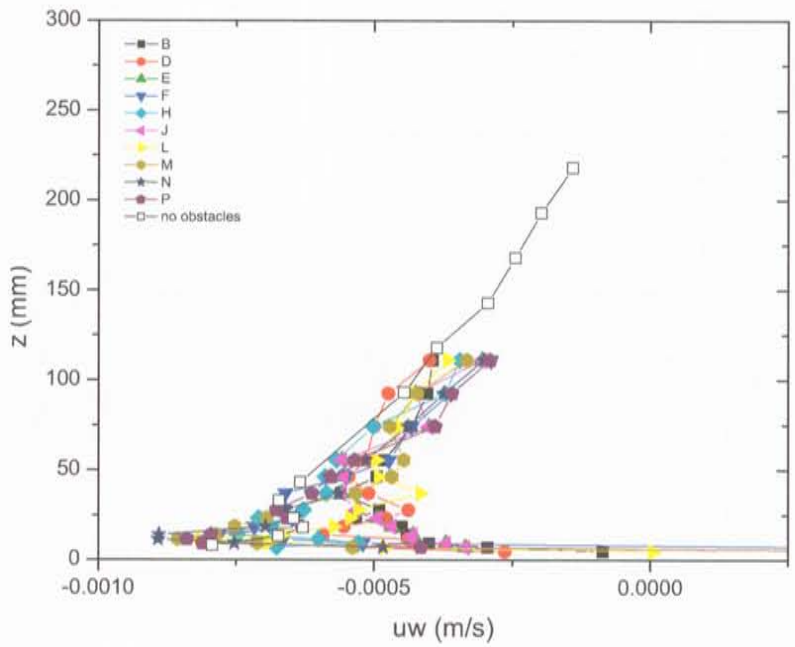

(b)

Figure 24: MUST array Reynolds stresses (a) uv at points A through H on the array centreline (b) uw at points B through P.

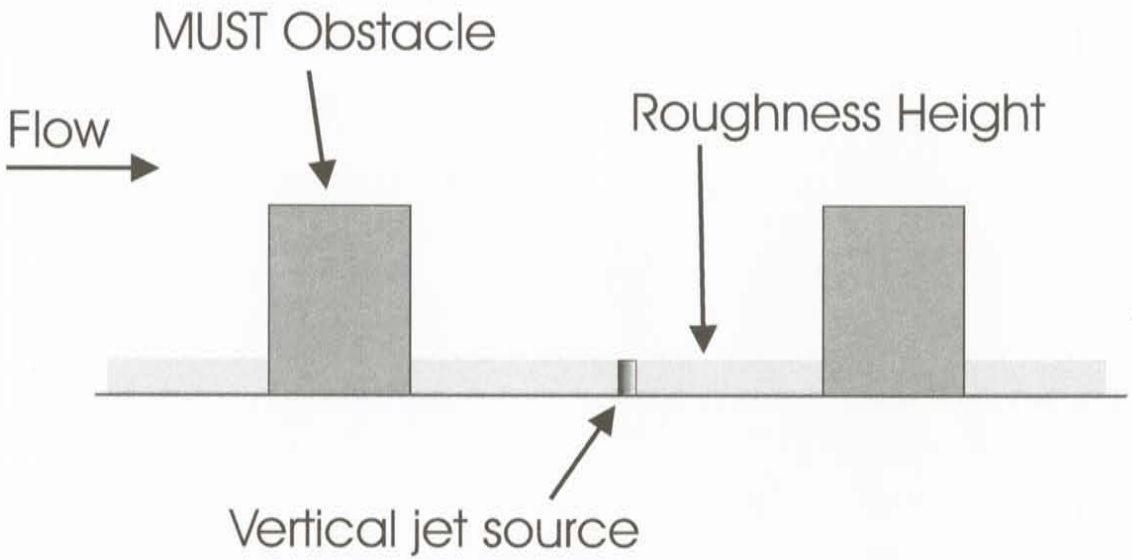

Figure 25: Vertical jet source 2.8 mm ID mounted in the MUST array between rows of obstacles.

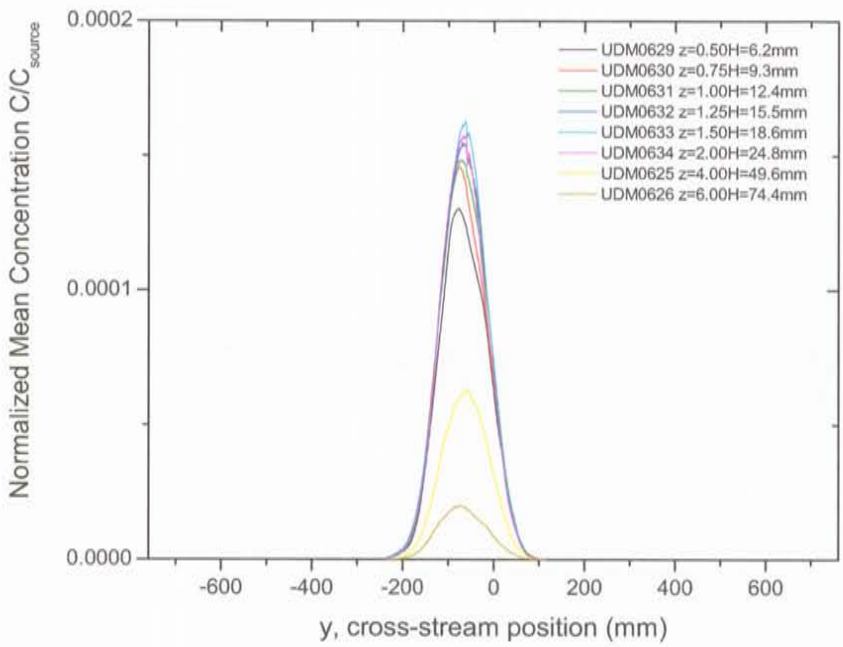

(a)

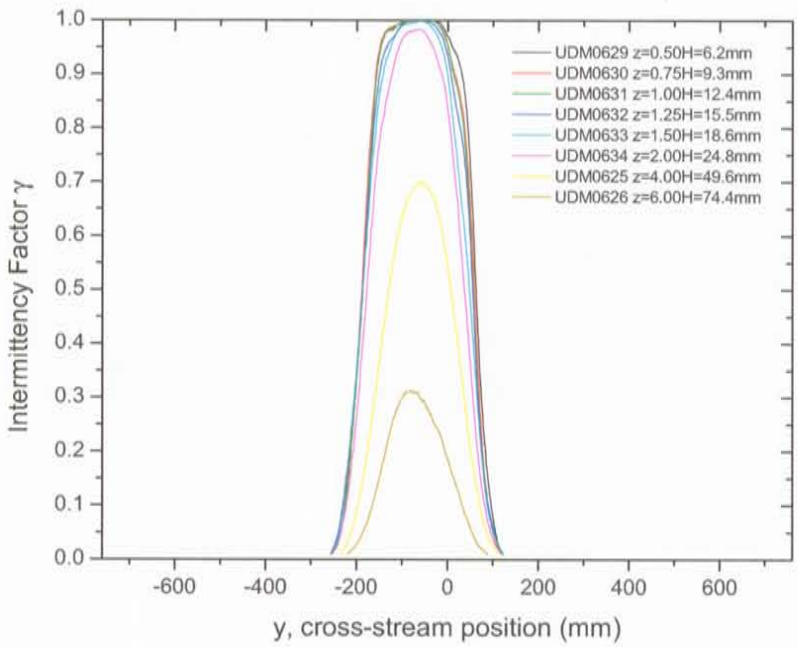

(b)

Figure 26: MUST001 concentration statistics at 5 rows downstream of the source. (a) mean concentration C (b) intermittency factor γ

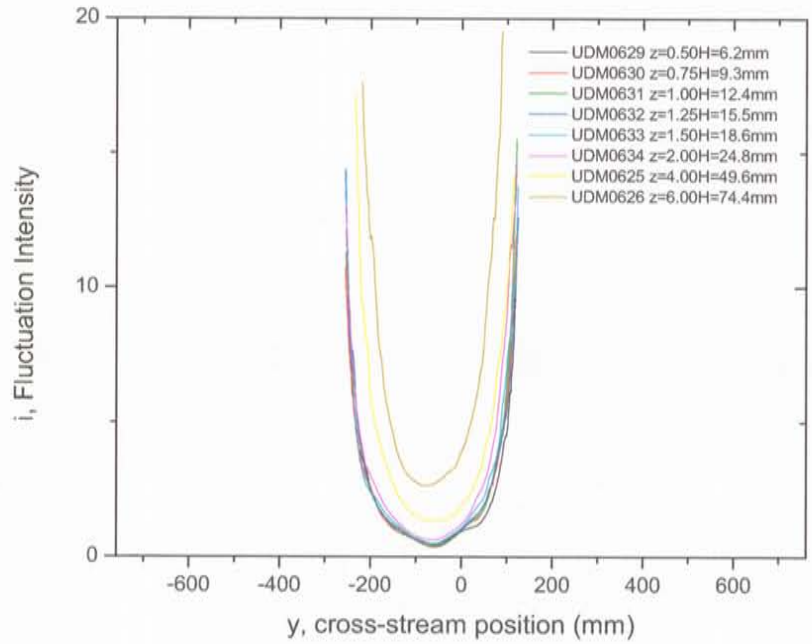

(a)

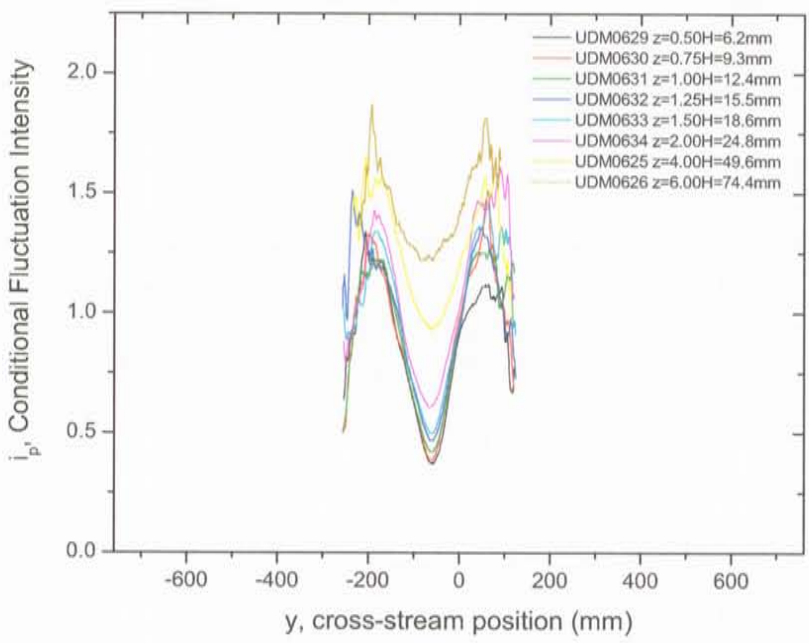

(b)

Figure 27: MUST001 concentration statistics at 5 rows downstream of the source. (a) fluctuation intensity i (b) conditional fluctuation intensity i_p

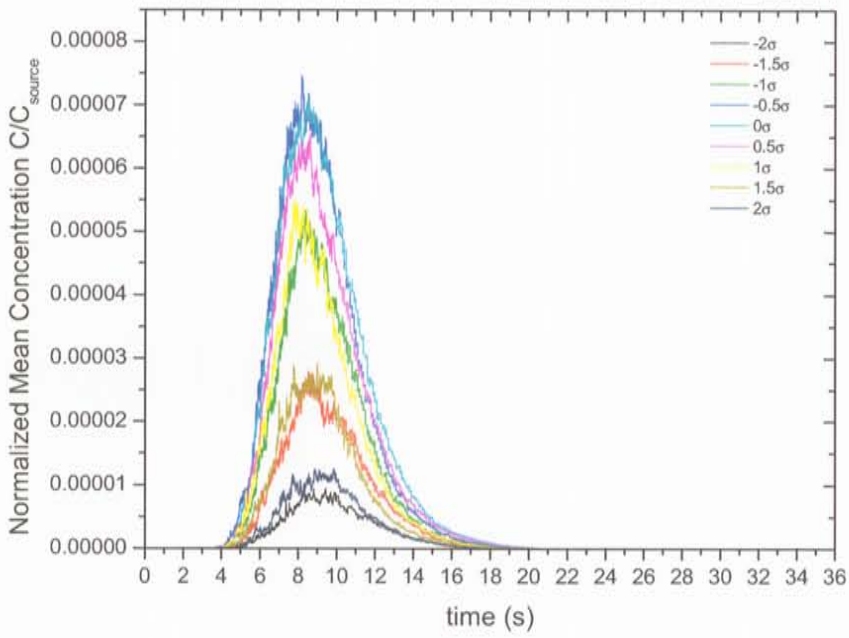

(a)

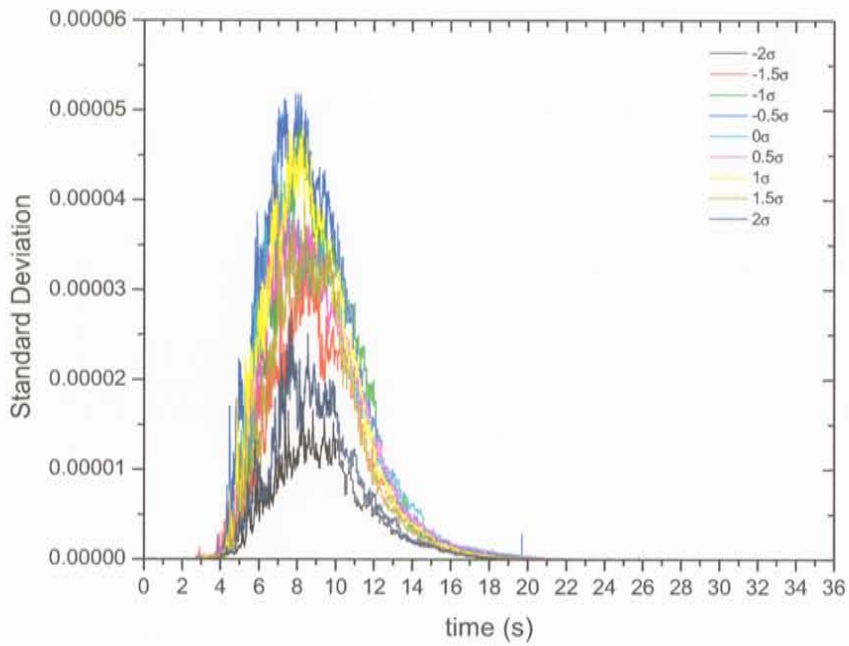

(b)

Figure 28: MUST007 ensemble puff concentration statistics as a function of time along a horizontal line at $z = 0.75H$, 5 rows downstream of the source, for a range of cross-stream positions. (a) Ensemble mean puff concentration. (b) Ensemble puff concentration standard deviation.

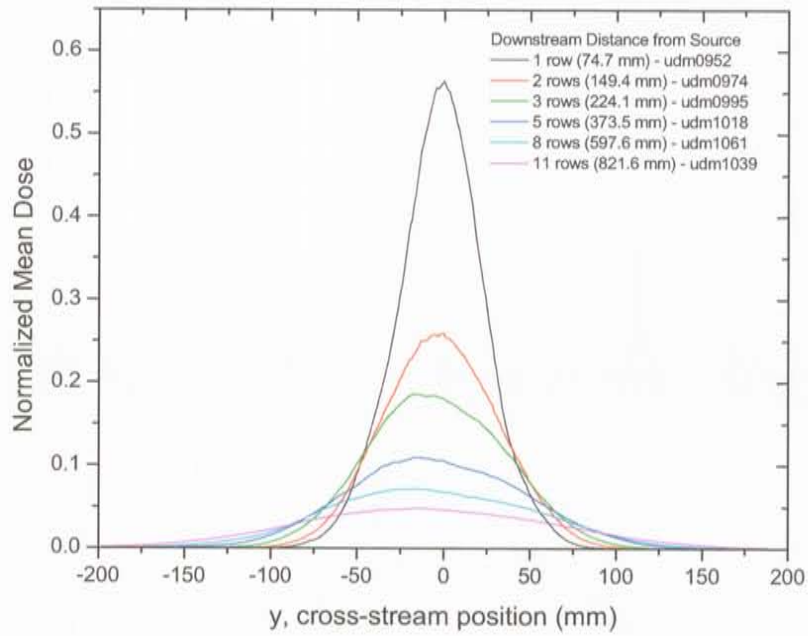

(a)

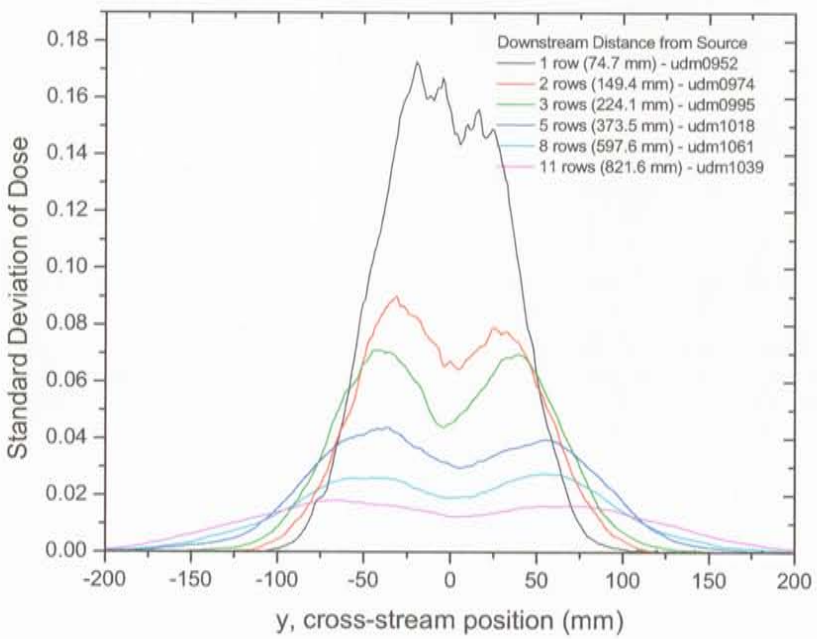

(b)

Figure 29: MUST007 puff dose statistics as a function of cross-stream position along a horizontal line at $z = 0.75H$. (a) Ensemble mean puff dose. (b) Ensemble puff dose standard deviation.

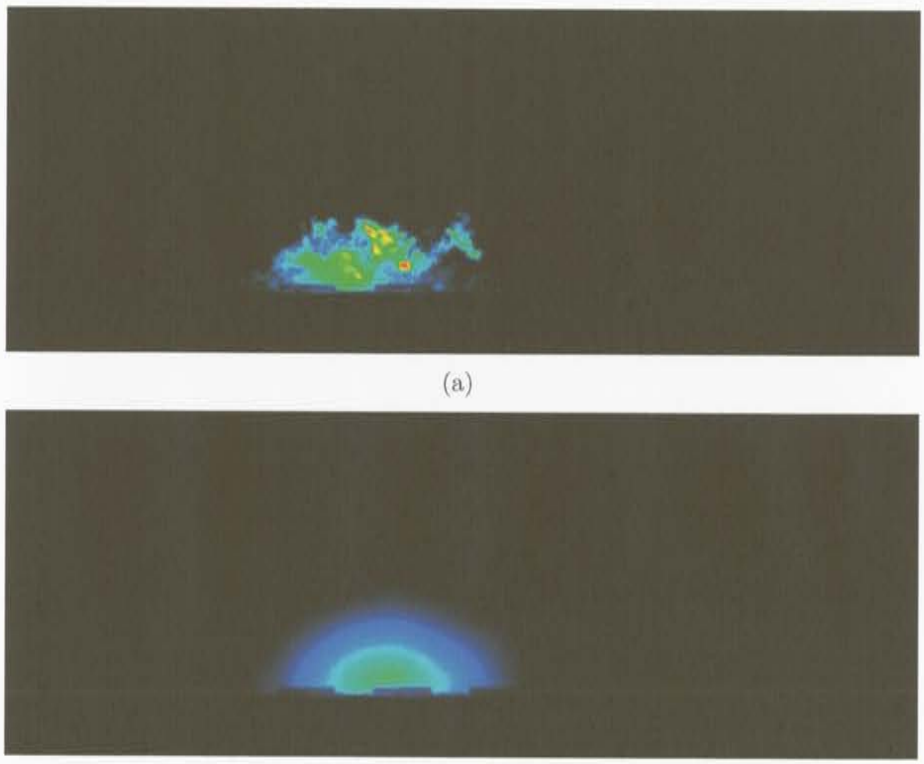

(a)

(b)

Figure 30: Sample 2-D concentration profiles on a $y - z$ plane 5 rows downstream of the source in the MUST array. (a) instantaneous plume cross-section (b) average concentration profile.

5 Urban Arrays

Following the MUST array tests, it was decided that a more flexible array design was needed so that changes to obstacle positions and sizes could be easily evaluated. Unlike the MUST array, there was no need to match any particular scale or aspect ratio for this new set of experiments, so Lego™ blocks were selected to provide a very flexible method of constructing arrays that could be easily changed between experiments.

The initial costs of Lego™ were similar to having individual obstacles machined from aluminum, but there were substantial savings in constructing alternative array configurations and altering the obstacles sizes without having to machine completely new obstacles. Several clear acrylic obstacles were also fabricated to match the size of the Lego™ obstacles for use in cases where the obstacle had to be transparent for optical measurement purposes.

The basic unit dimension for the urban arrays was 1.25" (31.75 mm = $1H$) based on the most convenient size of Lego™ available and the requirement to get a sufficiently large array in the water channel. Each cell in the array was a 2 unit square consisting of 4 quadrants as shown in Figure 31. An obstacle may be placed in any of the quadrants.

Figure 32 is a schematic top view of the 16×16 cell array layout used in the water channel. The cross-stream centerline of the channel is at a joint between 2 unit cells. Looking in the flow direction, columns on the right side of the centerline are numbered from -1 to -8 and on the left side from 1 to 8. In the flow direction, the rows are numbered 1 to 16. This numbering system allows any cell positions to be referred by a coordinate pair. For example cell (-2,3) is the second unit cell to the right of the centerline and the third unit cell downstream. The red dots in Figure 32 are the positions of holes that were drilled for dye release sources. Figure 33(a) is a close up of a single $1H$ Lego obstacle and Figure 33(b) is a photo of the entire 16x16 regularly spaced array in the water channel. All obstacles were mounted on Lego™ baseplates with no additional roughness around the obstacles.

The water channel flow configuration for the Urban arrays was exactly the same as for the MUST array. The same black expanded metal roughness was placed in the water channel upstream of the obstacle array. No expanded metal was placed around the obstacles for the Urban array tests, so the only roughness in the vicinity of the obstacle was the bumps on the Lego™ base plate which are approximately 2 mm high and 4.5 mm in diameter. and no changes were made to the inlet flow conditioning or the operating depth of the water channel.

5.1 Urban Array - 1D Linescan LIF

The dye source for all of the concentration measurements was a small diameter vertical jet source made from a 3.1 mm OD, 2.8 mm ID stainless steel tube, the same as used in the MUST array. The source flow rate was 12 ml/min. For the ground level releases the top of the source was at level with the tops of the Lego™ bumps at $z = 2$ mm. Some tests were made with elevated sources at $z = 1H = 31.75$ mm or $z = 2H = 63.5$ mm.

The concentration statistics calculated from these measurements are described in Section C. The array types were given a number in the sequence they were tested. Sample concentration statistics from measurements in UrbanArray001 are shown in Figures 34 and 35.

Basic descriptions of each of the arrays are listed below:

UrbanArray001 regular array of $1H$ obstacles. Several source positions were tested in this array configuration.

- Quadrant D behind an obstacle. Sample Figures 34 and 35 are from these measurements.
- Quadrant C between obstacles
- Quadrant D, but 8 rows downstream in the array
- elevated source at $z = 1H$ on top of an obstacle
- elevated source at $z = 2H$ on top of an obstacle

UrbanArray002 staggered array of $1H$ obstacles, with the source in quadrant C or D

UrbanArray003 regular array of $2H$ obstacles with the source in quadrant C or D

UrbanArray004-009 random height, regular arrays

UrbanArray010 alternating rows of $2H$ and $3H$ obstacles

UrbanArray011 regular $1H$ array with a single $3H$ obstacle downstream of the source

UrbanArray012 regular $1H$ array with a single $3H$ obstacle upstream and downstream of the source

UrbanArray013 regular $1H$ array with a single $3H$ obstacle upstream and two $3H$ obstacles downstream of the source

UrbanArray014 regular $1H$ array with a single $3H$ obstacle upstream of the source

UrbanArray015 regular $1H$ array with a single $3H$ obstacle upstream of the measurement position at 8 rows downstream.

UrbanArray016 regular $1H$ array with a single $3H$ obstacle downstream of the measurement position at 8 rows downstream.

UrbanArray017 regular $1H$ array with a $3H$ obstacle upstream and downstream of the 8 rows downstream measurement position

UrbanArray018 random placement of $1H$ obstacles, one obstacle per unit cell

UrbanArray019 same as array018 except for removal of obstacle immediately upstream of the source

UrbanArray020 random placement of $1H$ obstacles, one obstacle per unit cell, different from array018

UrbanArray021 random placement of $2H$ obstacles, one obstacle per unit cell, same configuration as UrbanArray020, but with taller obstacles

UrbanArray022 regular $1H$ array with the source 8 rows downstream in the array and a single $3H$ obstacle upstream of the source

UrbanArray023 regular $1H$ array with the source 8 rows downstream in the array and a single $3H$ obstacle downstream of the source

UrbanArray024 regular $1H$ array with the source 8 rows downstream in the array and a single $3H$ obstacle 2 rows downstream of the source

UrbanArray025 regular $1H$ array with the source 8 rows downstream in the array and a single $3H$ obstacle 3 rows downstream of the source

UrbanArray026 regular $1H$ array with the source 8 rows downstream in the array and a single $3H$ obstacle 4 rows downstream of the source

UrbanArray027 regular $1H$ array with the source 8 rows downstream in the array and a single $3H$ obstacle 2 rows upstream of the source

UrbanArray028 regular $1H$ array with the source 8 rows downstream in the array and a $3H$ obstacle upstream and downstream of the source

UrbanArray029 staggered array of 1H obstacles with an elevated source at $z = 1H$ or $z = 2H$

UrbanArray030 regular $1H$ array with row 4 shifted in the y direction by $-0.25H$

UrbanArray031 regular $1H$ array at 30° angle to the flow

UrbanArray032 staggered $1H$ array at 30° angle to the flow

UrbanArray033 regular $2H$ array at 30° angle to the flow

UrbanArray034 staggered $2H$ array at 30° angle to the flow

UrbanArray035 staggered $2H$ array at 45° angle to the flow

UrbanArray036 regular $2H$ array at 45° angle to the flow

UrbanArray037 regular $1H$ array at 45° angle to the flow

UrbanArray038 staggered $1H$ array at 45° angle to the flow

5.2 Urban Array Velocity Measurements

Several of the urban array configurations were selected for velocity measurement to complement the approach flow information available from the MUST array testing. The arrays and points chosen were selected to give a survey of the range of flow field conditions that could be expected inside the urban arrays. Samples of velocity statistics measured in UrbanArray001 are shown in Figures 36 to 38. The following velocity measurements were made:

UrbanArray001 regular array of 1H obstacles. Measurement positions were placed around an obstacle in the first row and the sixth row of the array. Sample Figures 36 to 38 are taken from these experiments.

UrbanArray002 staggered array of $1H$ obstacles. Measurement positions were placed around an obstacle in the first row and the sixth row of the array

UrbanArray003 regular array of $2H$ obstacles. Measurements were made around an obstacle in the first row, the sixth row and the twelfth row in the array.

UrbanArray027 regular $1H$ array with source 8 rows downstream in the array and a single $3H$ obstacle 2 rows upstream of the source. Velocity measurements were made around the source position.

UrbanArray028 regular $1H$ array with source 8 rows downstream in the array and a $3H$ obstacle upstream and downstream of the source. Velocity measurements were made around the source position.

UrbanArray031 regular $1H$ array at 30° angle to the flow. Measurements were made around an obstacle in the sixth row of the array.

UrbanArray032 staggered $1H$ array at 30° angle to the flow. Measurements were made around an obstacle in the sixth row of the array.

UrbanArray037 regular $1H$ array at 45° angle to the flow. Measurements were made around an obstacle in the sixth row of the array.

UrbanArray038 staggered $1H$ array at 45° angle to the flow. Measurements were made around an obstacle in the sixth row of the array.

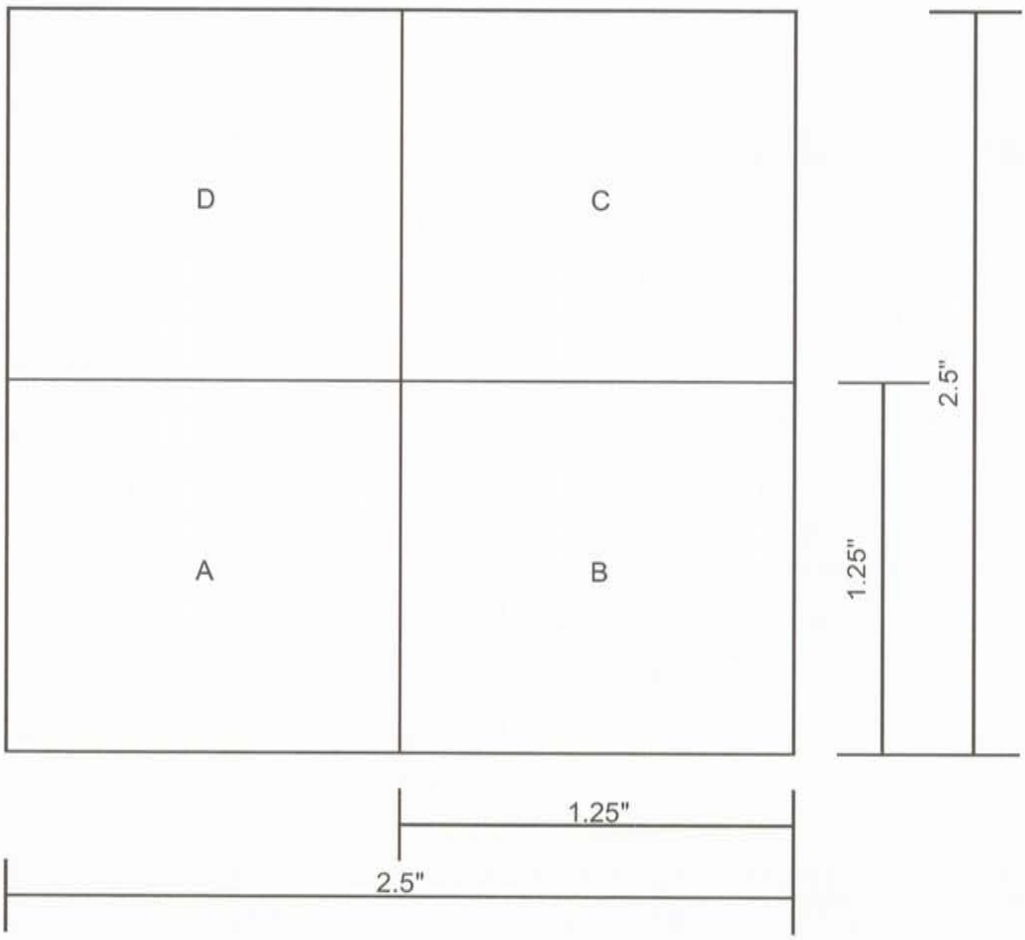

Figure 31: Basic unit cell arrangement and dimensions for the urban arrays. Obstacles could be placed in any of the 4 quadrants A through D in the unit cell. The base dimension was the unit obstacle height $H = 1.25$ in $= 31.75$ mm. Each unit cell was $2H$ x $2H$.

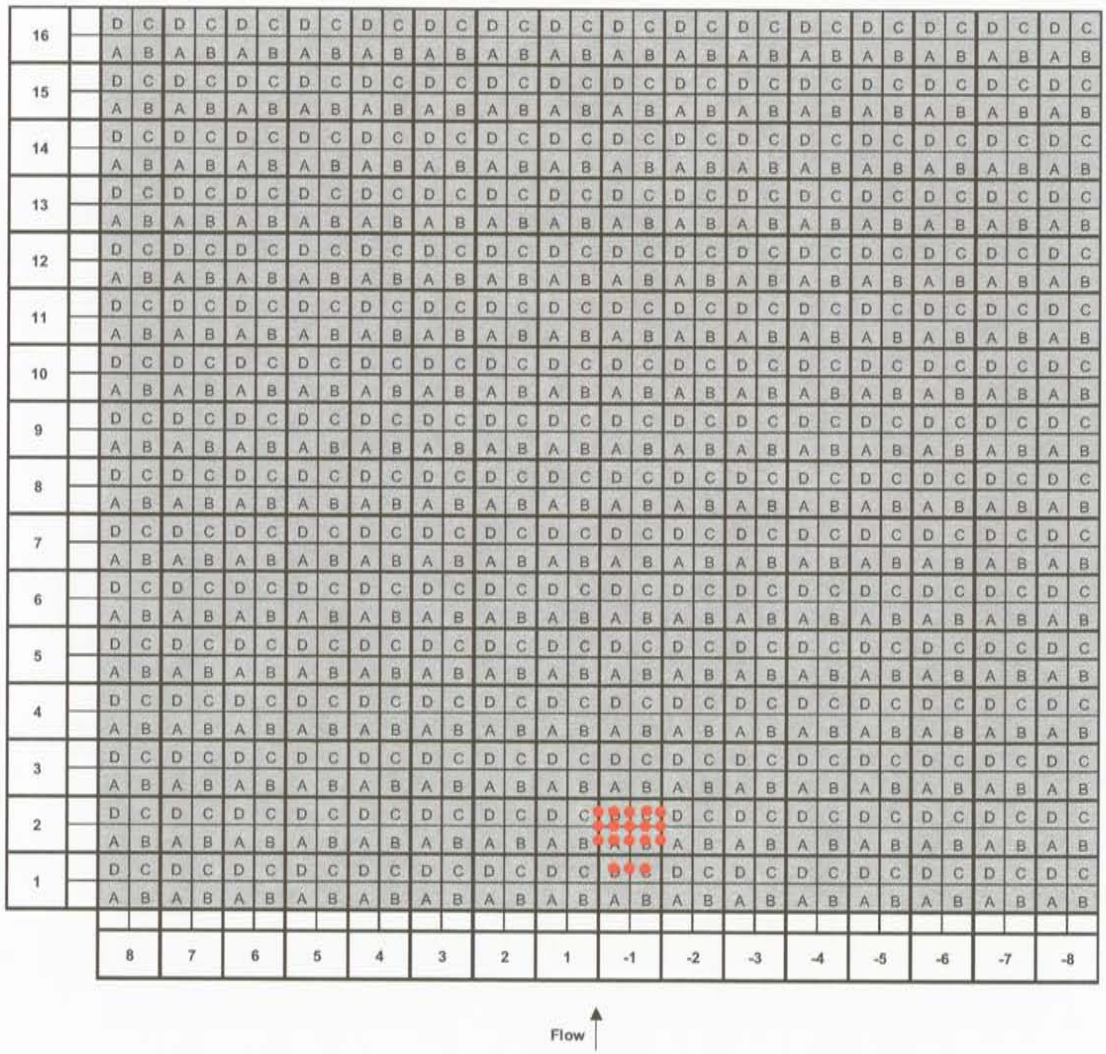

Figure 32: Arrangement of 16 × 16 unit cell urban array showing the unit cell numbering system. Obstacles could be placed in any of the 4 quadrants A through D in the unit cell. The red dots were holes drilled in the panel for source locations.

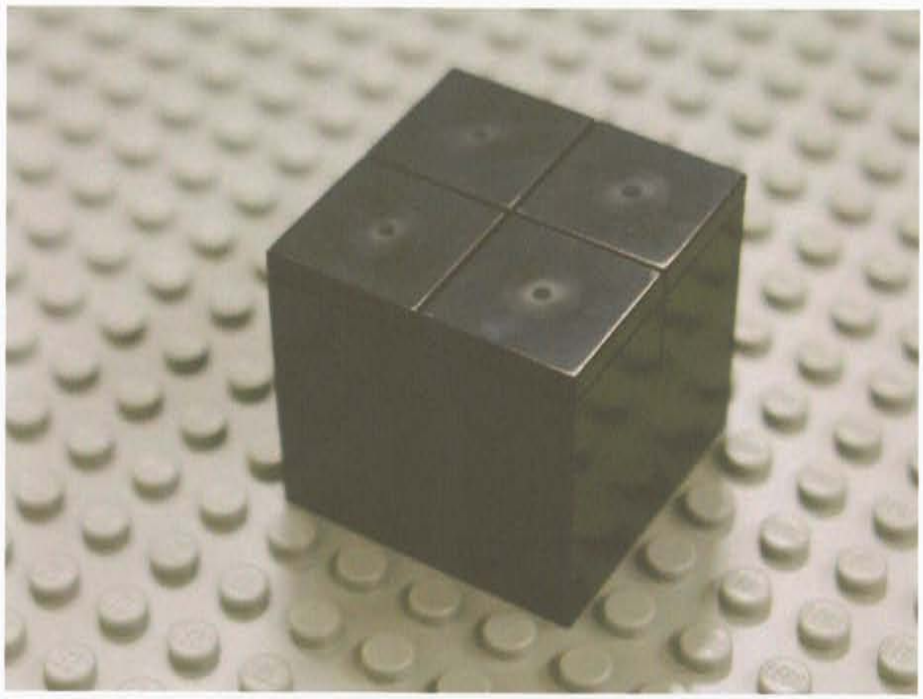

(a)

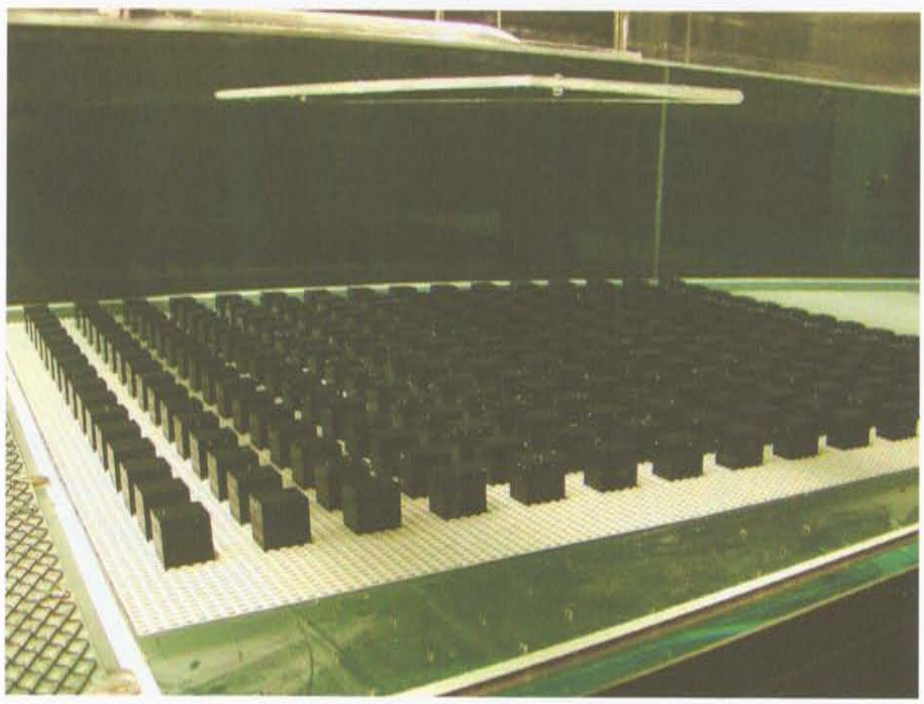

(b)

Figure 33: (a) A single $1H \times 1H \times 1H$ Lego obstacle. (b) Regularly spaced 16×16 $1H$ obstacle array.

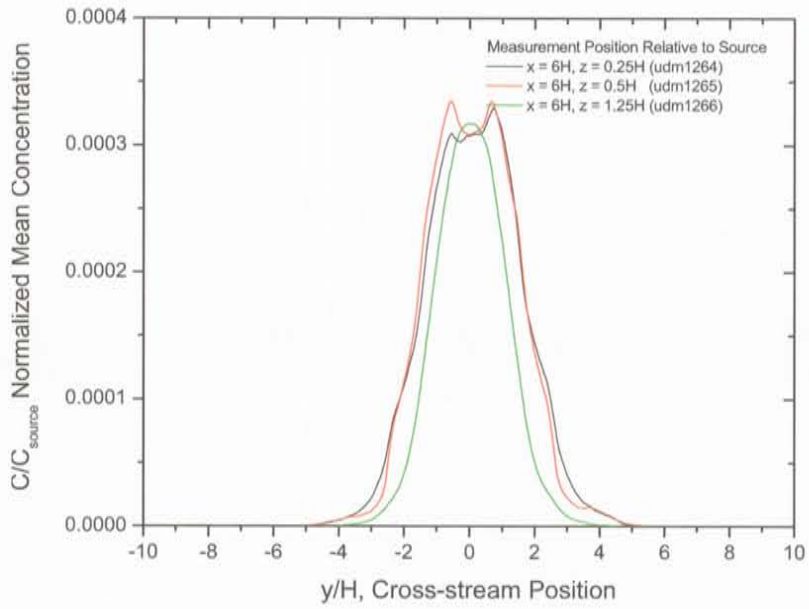

(a)

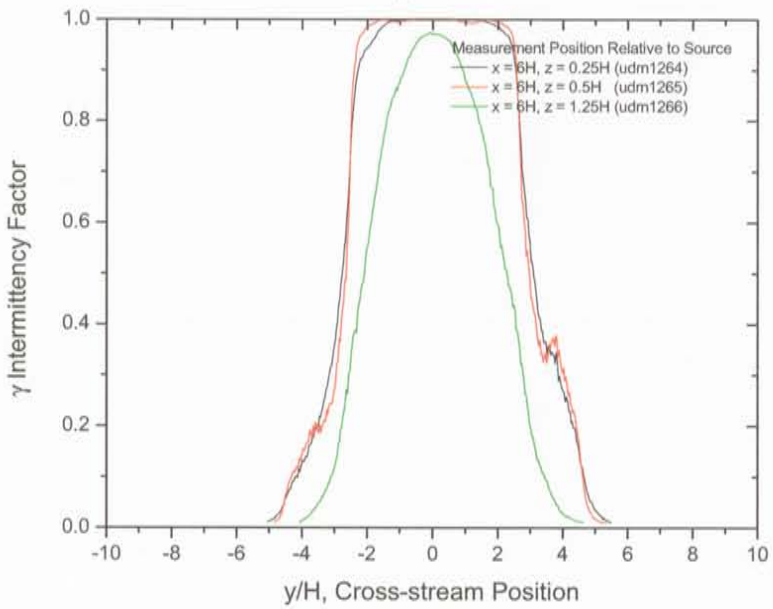

(b)

Figure 34: Concentration statistics at $6H = 190.5$ mm downstream of the source in UrbanArray001 regularly spaced $1H$ obstacles with ground level source in quadrant D. (a) mean concentration C (b) intermittency factor γ

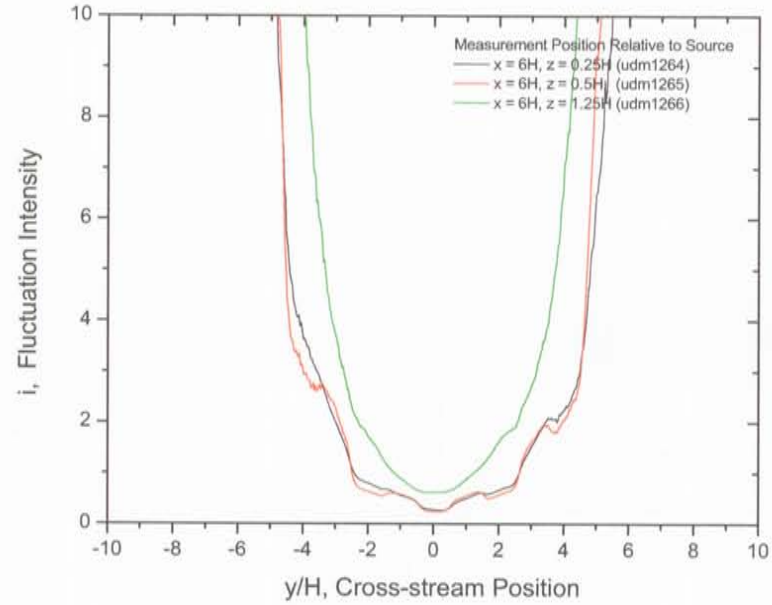

(a)

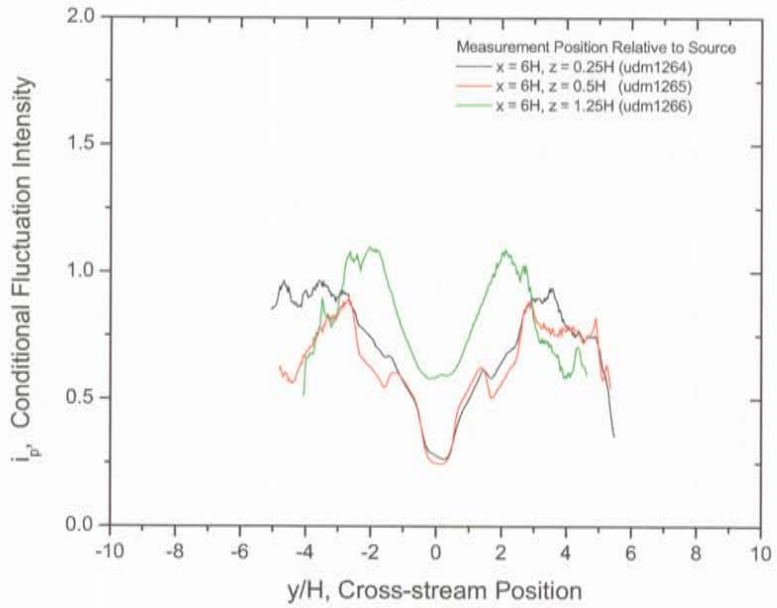

(b)

Figure 35: Concentration statistics at $6H = 190.5$ mm downstream of the source in UrbanArray001 regularly spaced $1H$ obstacles with ground level source in quadrant D. (a) fluctuation intensity i (b) conditional fluctuation intensity i_p

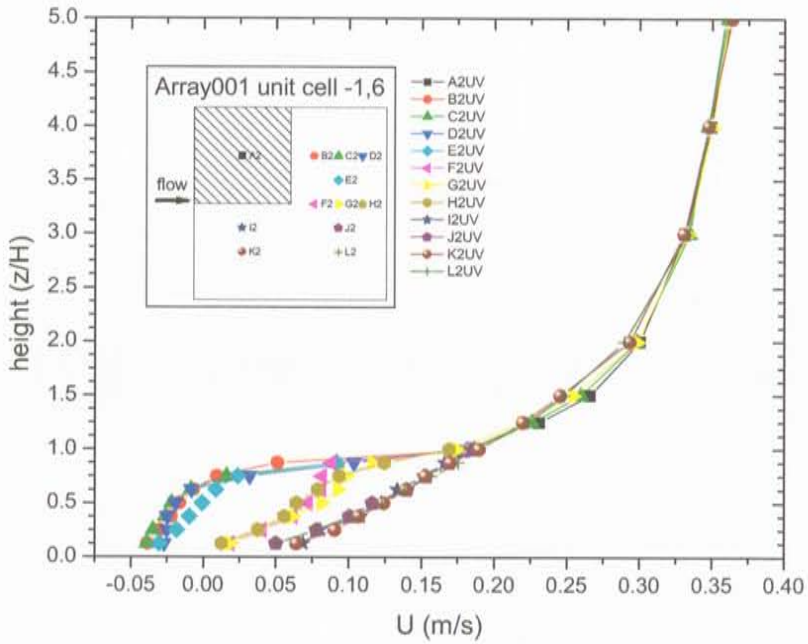

(a)

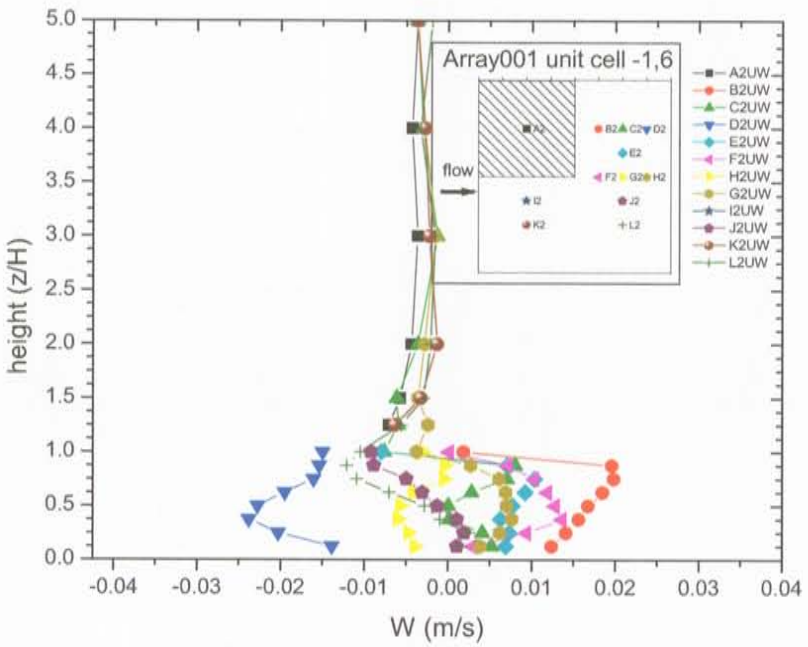

(b)

Figure 36: UrbanArray001 velocity profiles in the 6th downstream unit cell (a) streamwise mean velocity U (b) vertical mean velocity W.

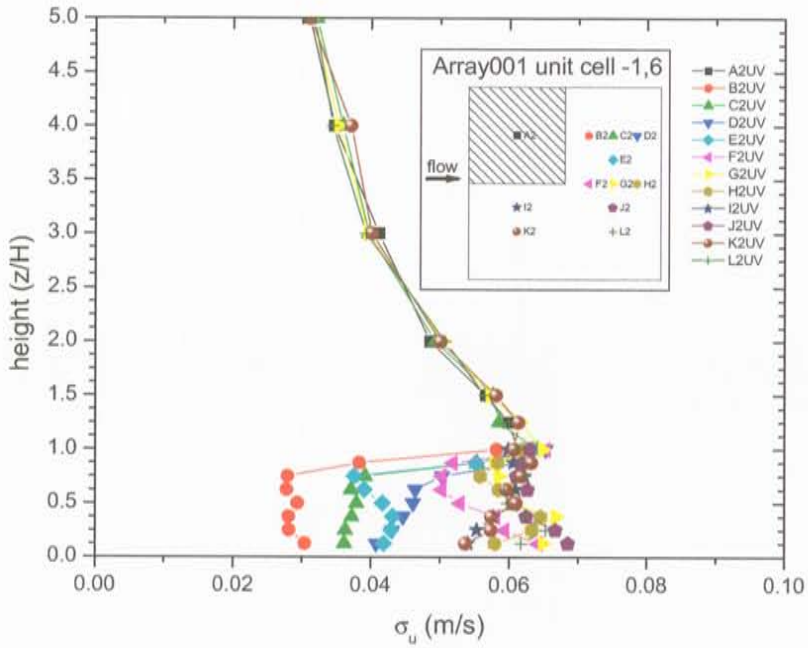

(a)

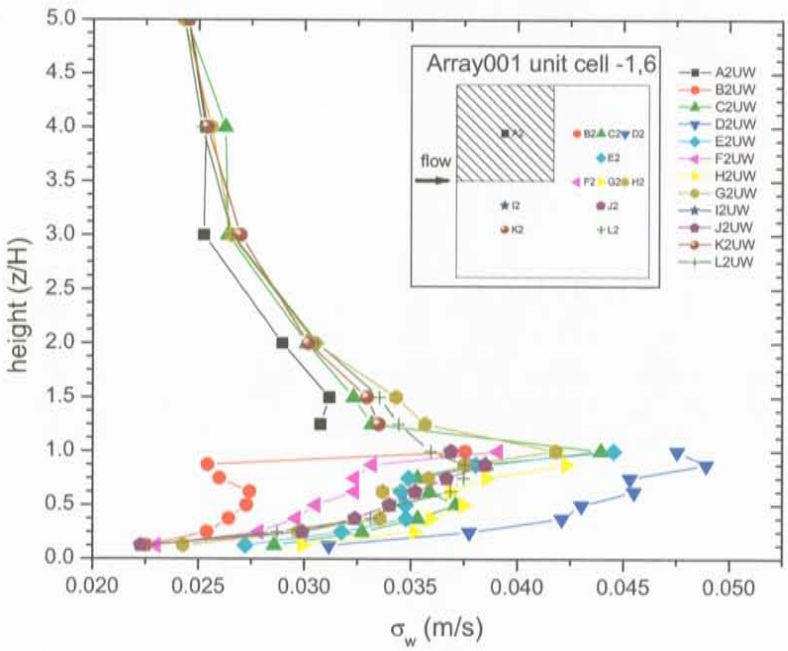

(b)

Figure 37: UrbanArray001 velocity profiles of velocity standard deviation in the 6th downstream unit cell (a) streamwise velocity component σ_u (b) vertical velocity component σ_w.

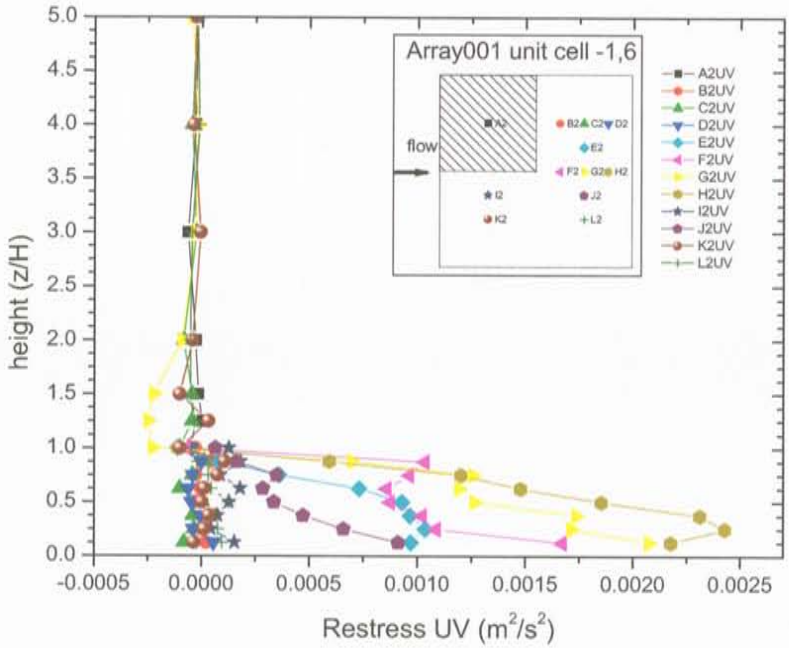

(a)

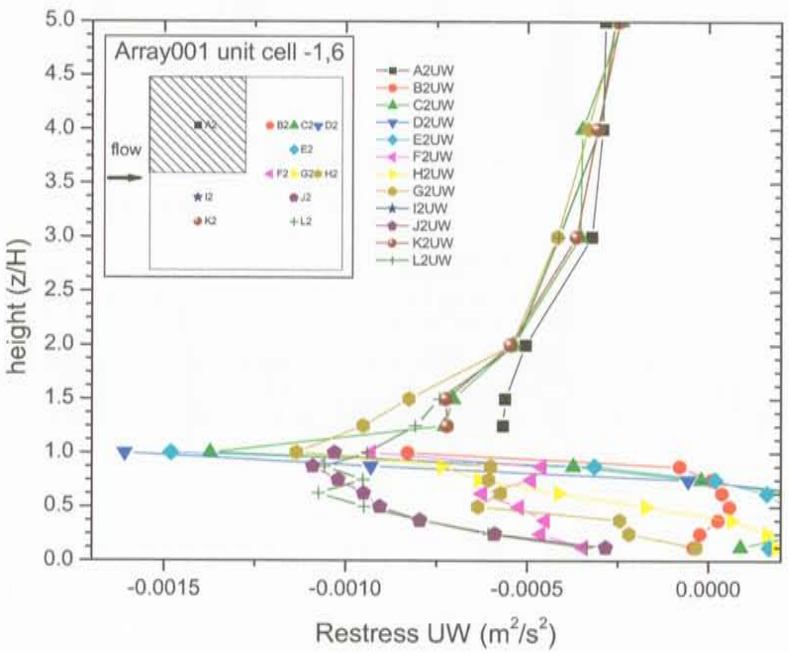

(b)

Figure 38: UrbanArray001 Reynolds stresses (a) $\overline{u'v'}$ (b) $\overline{u'w'}$.

A General Data File Notes

The following software versions were used to compile the data files and documentation:

- Adobe Acrobat Version 6.0 (`*.pdf`)
- Microsoft Excel Version 9.0 - Office 2000 (`*.xls`)
- OriginLab Origin Version 6.1 (`*.OPJ`)
- WinZip Version 8.1 was used to compress many of the large files (`*.zip`). The zip algorithm is widely used and many other zip/unzip programs should be able to work with these compressed files.

All of the data collection and analysis programs used to generated the data and reduced data files were written by Coanda employees. These programs are not attached to this report nor are they necessary for any further analysis. Appendices B and C discuss the methods of calculation and the file formats.

The CD's accompanying this report include all of the plots and Excel summary files of the measurement statistics. The CD's also contain additional reduced data files in standard comma separated variable ASCII text files (`*.csv`) that have been processed, but were not plotted or pasted into Excel workbooks. All of the raw concentration and velocity measurement data are available for additional processing.

Each data set collected (velocity or concentration data) was named with the prefix `udm####`. The `udm` indicates that is was part of the Coanda urban dispersion modelling project and the `####` is a four digit run number. The suffix and extension indicates the data and file type.

Each data set was numbered sequentially as it was collected. Please note that there are many runs excluded from this final compilation because they were calibrations, test runs, or in some cases experiments that were deleted when errors were discovered after collection and analysis.

B Velocity Data

B.1 Velocity Statistics

Velocity statistics were calculated with the TSI FIND Program Version 4.0 and then compiled into spreadsheets and graphs. The velocity component definitions presented below were taken from Appendix B of the FIND Manual. All velocity measurements were collected with 500 second sample times at each position.

The LDV measured two components of velocity simultaneously. For each of the velocity components, VEL1 and VEL2, the following statistics were calculated (for demonstration purposes VEL1=u and VEL2=w):

total points total number of measurements, N, obtained at that position over the total sampling time t_s.

mean, m/s U is the mean velocity in the streamwise, x, direction

$$U = \frac{\sum u}{N} \tag{2}$$

standard deviation, m/s σ_u is the standard deviation of velocity fluctuation

$$\sigma_u = \sqrt{\frac{\sum u^2}{N} - U^2} \tag{3}$$

turbulence intensity, % the standard deviation of velocity fluctuation σ_u as a percentage of the mean velocity U at that position.

$$\text{turbulence intensity (\%)} = \frac{\sigma_u \times 100}{U} \tag{4}$$

third moment, $\mathrm{m}^3/\mathrm{s}^3$

$$\text{third moment} = \frac{\sum u^3}{N} - \left(3 \times \frac{\sum u^2}{N} \times U\right) + 2U^3 \tag{5}$$

skewness coefficient

$$\text{skewness coefficient} = \frac{\text{third moment}}{2\sigma_u^3} \tag{6}$$

fourth moment, $\mathrm{m}^4/\mathrm{s}^4$

$$\text{fourth moment} = \frac{\sum u^4}{N} - \left(4 \times \frac{\sum u^3}{N} \times U\right) + \left(6 \times U^2 \times \frac{\sum u^2}{N}\right) - 3U^4 \tag{7}$$

flatness coefficient

$$\text{flatness coefficient} = \frac{\text{fourth moment}}{\sigma_u^4} \tag{8}$$

The same set of statistics and calculations applies for the VEL2=w component. The final columns in the spreadsheet are the cross-correlation components VEL1VEL2=uw

total points total number of measurements, N, obtained at that position over the total sampling time t_s. This will be the same number as the total points for VEL1 and VEL2

velocity projection, m/s vector sum of the two orthogonal measured components u and w.

$$\text{velocity projection} = \sqrt{u^2 + w^2} \tag{9}$$

mean velocity angle, degrees direction of the velocity projection in the $x - z$ plane where the x-axis would be at 0 degrees and the angle is measured counter-clockwise from the x-axis.

$$\begin{aligned}
\text{angle} &= \arctan(w/u) && \text{if } (u > 0) && (10)\\
&= \pi + \arctan(w/u) && \text{if } (u < 0) && (11)\\
&= \pi/2 && \text{if } (u = 0 \text{ and } w > 0) && (12)\\
&= 3\pi/2 && \text{if } (u = 0 \text{ and } w < 0) && (13)
\end{aligned}$$

Reynolds Stress, m^2/s^2

$$\overline{u'w'} = \overline{uw} - \overline{u} \times \overline{w} \tag{14}$$

correlation coefficient

$$\text{correlation coefficient} = \frac{\overline{u'w'}}{\sigma_u \sigma_w} \tag{15}$$

All of these velocity statistics are tabulated in Excel workbooks.

B.2 Velocity Binary Data Files

All of the velocity measurements made with the LDV were compiled into binary files that can be used for further analysis. There are no headers on the files, they are simply binary lists of the two velocity components measured for each sample collected by the LDV. The information is stored as 4 byte (32 bit) single precision floating point numbers in the standard Intel "Little-Endian" binary format. Each velocity measurement in the file consists of 3 values:

- the first value is the VEL1 velocity in m/s

- the second value is the VEL2 velocity in m/s
- the third value is the time between the current sample and the previous sample in microseconds.

Note that for the first entry in the file, the time data is meaningless because there is no previous sample for comparison.

As an example, consider the data in the Raupach velocity binary file `VEL-0001-001.BIN`. The total length of this file is 479,232 bytes so it contains 479,232/12 = 39,936 velocity measurements. The first 24 bytes in the file are the first two velocity measurements as given below:

Byte #	Hexadecimal Value	Decimal Value	Description
0-3	be 6d 72 3a	0.000925	sample #1 VEL1 (m/s)
4-7	ca 22 22 bc	-0.009896	sample #1 VEL2 (m/s)
8-11	00 a0 2e 4c	45776896.0	time between data (μs), meaningless for the first sample
12-15	72 f7 ec bb	-0.007232	sample #2 VEL1 (m/s)
16-19	44 42 b9 b9	-0.000353	sample #2 VEL2 (m/s)
20-23	00 00 79 46	15936.0	time between sample #1 and #2 (μs)
⋮	⋮	⋮	⋮

C Concentration Data

C.1 Reduced Data Files and Statistic Definitions

All concentration statistics were calculated with dimensionless concentrations where the measured concentration was normalized by the source concentration C_{source}. These normalized values can also be interpreted as the concentration produced by a source concentration of 1 unit. The concentration unit can be whatever type of concentration units one would like to use. For example if one would like the concentration in parts per million (ppm), simply take the dimensionless concentration value given in the statistics files and multiply by 10^6. In the notation below, c is the normalized concentration at any single sample and C is the normalized mean concentration. For clarity the normalizing factor C_{source} will not be shown in any of the equations or discussion below.

Note that the actual experimental source dye concentration was changed for each measurement to ensure that the fluorescence intensity was within the range of the camera at each downstream position. This real source concentration value in recorded in the Excel spreadsheet files with the suffix `*ConcSum.xls` for future reference.

All of the data in the `reduced_data` directories are stored as comma separated variable ASCII files denoted by the extension `*.csv`. These should be easily read by almost any data analysis program and can also be viewed or edited with any text editor. The first line of each file is a header line naming each column of data. The file type is described by the suffix added to the root data file name `udm####`.

The definitions of variance, skewness and kurtosis and the corrected two-pass algorithm used to calculate the values were taken from Press et al. (1992).

C.1.1 Concentration Statistics `*stats.csv` and `*stat.xls`

Basic concentration statistics for each pixel across the plume. The data columns are:

pixel linescan camera pixel number

x, y, z positions of each pixel relative to the source in the x and y coordinates and relative to the ground for the z coordinate. (i.e. x = x_line-x_source, y = y_line-y_source, z = z_line)

x_line, y_line, z_line positions of each pixel relative to the array reference position (mm)

x_source, y_source, z_source position of the source relative to the array reference position (mm)

mean normalized mean concentration, C

$$C = \frac{1}{N}\sum_{j=1}^{N} c_j \tag{16}$$

(17)

where N is the number of samples.

condmean conditional (in-plume) mean concentration, C_p, calculated by excluding all of the zero concentration measurements

$$C_p = \frac{C}{\gamma} \tag{18}$$

$$\tag{19}$$

dilution inverse of normalized mean concentration, $1/C$

gamma intermittency factor γ fraction of time the concentration was greater than zero; in other words it is the probability of observing a measurable concentration.

i fluctuation intensity i = standard deviation of concentration / mean concentration

$$i = \frac{\sigma_c}{C} \tag{20}$$

$$\tag{21}$$

i2 fluctuation intensity squared i^2 = variance of concentration / mean concentration squared

ip conditional fluctuation intensity = standard deviation of non-zero concentrations / conditional mean concentration

$$i_p = \frac{\sigma_{c_p}}{C_p} \tag{22}$$

$$\tag{23}$$

ip2 conditional fluctuation intensity squared i_p^2 = variance of non-zero concentrations / conditional mean concentration squared

sdev standard deviation of concentration σ_c

$$\sigma_c = \sqrt{\frac{1}{N-1}\sum_{j=1}^{N}(c_j - C)^2} \tag{24}$$

$$\tag{25}$$

var variance of concentration = $\mathsf{sdev}^2 = \sigma_c^2$

skew concentration skewness

$$\mathsf{skew} = \frac{1}{N}\sum_{j=1}^{N}\left(\frac{c_j - C}{\sigma_c}\right)^3 \tag{26}$$

$$\tag{27}$$

kurtosis concentration kurtosis

$$\text{kurtosis} = \left[\frac{1}{N}\sum_{j=1}^{N}\left(\frac{c_j - C}{\sigma_c}\right)^4\right] - 3 \tag{28}$$

$$\tag{29}$$

second, third, fourth second, third and fourth moments of concentration around zero.

$$\text{second} = \frac{1}{N}\sum_{j=1}^{N} c_j^2 \tag{30}$$

$$\text{third} = \frac{1}{N}\sum_{j=1}^{N} c_j^3 \tag{31}$$

$$\text{fourth} = \frac{1}{N}\sum_{j=1}^{N} c_j^4 \tag{32}$$

C.1.2 Plume Spreads `*spread.csv`

Plume spreads and centroids for the first four moments of concentration. Columns in the data file are:

filename data file name `udm####`

centroid1 is the centroid of the mean concentration profile across the plume in units of mm relative to the source position. For horizontal linescan measurements it is sometimes referred as $\overline{y}$ and for vertical linescan measurements it is $\overline{z}$. For example, for most of the horizontal linescans $\overline{y}$ is close to zero, as expected, indicating that the centroid of the plume is very near the centroid of the source. For vertical linescans $\overline{z}$ is a positive number indicating that the centroid of the plume is above the source height as expected for ground level sources.

$$\overline{y} = \frac{\sum_{k=1}^{N_p} y_k C_k}{\sum_{k=1}^{N_p} C_k} \tag{33}$$

where N_p is the number of pixels measured across the plume (typically 1016), y_k is the position of pixel number k and C_k is the average concentration measured at pixel number k.

spread1 is the spatial variance of the mean concentration profile across the plume commonly referred to as the plume spread squared σ_y^2 for a horizontal line across the plume or σ_z^2 for a vertical line across the plume in units of mm^2.

$$\sigma_y^2 = \frac{\sum_{k=1}^{N_p} (y_k - \overline{y})^2 C_k}{\sum_{k=1}^{N_p} C_k} \tag{34}$$

centroid2, centroid3, centroid4 are the centroids of the second, third and fourth moments across the plume in units of mm relative to the source position.

$$\text{centroid2} = \frac{\sum_{k=1}^{N_p} y_k \text{second}_k}{\sum_{k=1}^{N_p} \text{second}_k} \tag{35}$$

$$\text{centroid3} = \frac{\sum_{k=1}^{N_p} y_k \text{third}_k}{\sum_{k=1}^{N_p} \text{third}_k} \tag{36}$$

$$\text{centroid4} = \frac{\sum_{k=1}^{N_p} y_k \text{fourth}_k}{\sum_{k=1}^{N_p} \text{fourth}_k} \tag{37}$$

spread2, spread3, spread4 the squared plume spread of the second, third, and fourth moments of concentration across the plume in units of mm^2.

$$\text{spread2} = \frac{\sum_{k=1}^{N_p} (y_k - \text{centroid2})^2 \text{second}_k}{\sum_{k=1}^{N_p} \text{second}_k} \tag{38}$$

$$\text{spread3} = \frac{\sum_{k=1}^{N_p} (y_k - \text{centroid3})^2 \text{third}_k}{\sum_{k=1}^{N_p} \text{third}_k} \tag{39}$$

$$\text{spread4} = \frac{\sum_{k=1}^{N_p} (y_k - \text{centroid4})^2 \text{fourth}_k}{\sum_{k=1}^{N_p} \text{fourth}_k} \tag{40}$$

C.1.3 Power Spectra `*p####spec.csv` compressed into `*spec.zip`

Concentration power spectra evaluated for selected pixels where #### is the pixel number. The pixel numbers are selected by starting at the plume source centreline and finding the pixels closest to the positions on the centreline, ± 0.5, ± 1.0, ± 1.5, ± 2.0, ± 2.5, ± 3.0, ± 4.0 and ± 5.0 of the plume spread σ_y (or σ_z for vertical linescans). In many cases there is insufficient data to make calculations all the way out to $5.0\sigma_y$ and so some of the positions may be missing. Columns in the data files are:

freq frequency in Hz.

powspec E_c, is the one-dimensional power spectrum of concentration computed using the methods given in Press et al. (1992, Section 13.4). The power spectrum is calculated from the normalized concentration c/C_{source} as are all of the other statistics. The powspec values are sometimes called the power spectral density and have the units of $s \cdot (\text{concentration units})^2$. In this case, the concentration units are dimensionless so the spectral density has the units of seconds. The area under the powspec versus frequency plot is by definition equal to the variance of the concentration fluctuations. Hinze (1975) has some discussion of power spectra of turbulent fluctuations if more detail is required.

C.1.4 Integral Time Scales `*ts.csv`

Integral time scales of concentration for selected pixels. Pixels were selected as for the spectra files described above. Columns in the data files are:

pixel linescan camera pixel number

timescale integral time scale of concentration fluctuation, T_c defined as the area under the auto-correlation curve for the concentration time series. It is an indication of the average time scale of concentration fluctuations and the time over which the concentration remains correlated. Following Hinze (1975, pp. 62-65), the time scale can be calculated from a time series of data by computing the one-dimensional power spectrum. The zero frequency intercept $E_c(0)$ is found by extrapolation and applied to the definition:

$$T_c = \frac{E_c(0)}{4\mathsf{var}} \tag{41}$$

C.1.5 Probability Distributions `*p####df.csv` compressed into `*df.zip`

Probability distribution functions of concentration evaluated for pixels selected as for the spectra files where `####` is the pixel number. Columns in the data files are:

conc concentration level in dimensionless concentration units (c/C_{source}).

pdf is the probability density of concentration $p(c)$ calculated by dividing the total range of the concentration data into narrow bins and then counting the values that end up in each bin for each pixel measured. The probability P of observing a concentration between two values c_1 and c_2 is

$$P(c_1 < c < c_2) = \int_{c_1}^{c_2} p(c)\, dc \tag{42}$$

and the probability $P(0 \leq c < \infty) = 1.0$ by definition.

cdf cumulative probability function, $P(c < c_2)$

$$P(c < c_2) = \int_{0}^{c_2} p(c)\, dc \tag{43}$$

edf exceedance probability function, $P(c > c_1)$

$$P(c > c_1) = \int_{c_1}^{\infty} p(c)\, dc \tag{44}$$

C.2 Centroid Tracking and Removal of Plume Meander `*_instcnt*.*`

One of the interesting uses of the linescan data sets is to examine plume meandering directly by calculating the instantaneous centroid position for each linescan sample and then shifting all of the linescans so that their centroids are at the same position. In this way, the overall meandering movements of the plume are removed from the data set and it is equivalent to having the measurement instrument follow the centroid of the plume.

These calculations were performed by taking the raw concentration data, calculating the centroid position and then copying the data into a new file but shifted so that the instantaneous centroid is at pixel 1016 out of a new total of 2032 pixels. Figure 39 illustrates this process of finding the centroid and then shifting all of the linescans so that the centroids like up. The result of this process is an output data file that is twice the size of the original because there has to be enough room in the new file to capture the entire width of the plume. The concentration data files in this new format are called `udm####_instcnt.conc` and are in exactly the same format as the `*.conc` files described in Section C.3 except that each line is 2032 pixels wide instead of 1016.

In the `reduced_data` sub-directories there are files with `_instcnt` added to their names indicating that they have been calculated using the concentration files with their instantaneous plume centroids aligned, but the calculations are otherwise identical to those described in Section C.1.

The files named `udm####_instcntcntspr.csv` have four columns of information about the instantaneous plume measurements:

k measurement line number

centroid plume centroid position in pixels from the original `*.conc` concentration file.

mass sum of the integer concentration values across the instantaneous plume. This is a surrogate measure of the total mass of plume material passing through the measurement line at that instant.

spread instantaneous plume spread squared, σ_y^2 or σ_z^2 in units of pixels^2.

These files are zipped into `*_instcntcntspr.zip` files to conserve space.

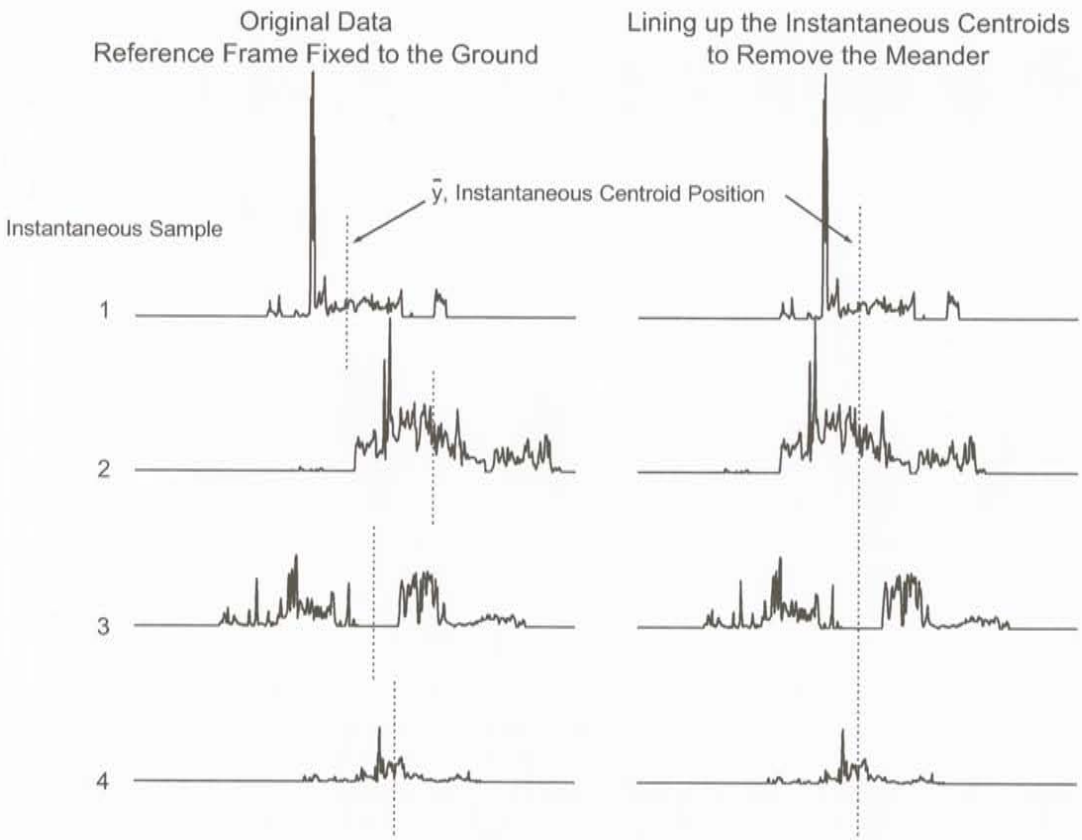

Figure 39: Illustration of the process used to remove the plume meandering and produce the data in the `*_instcnt.conc` files.

C.3 Binary Concentration Files *.conc

Inside each *conc.zip file is a *.conc file which is binary concentration data in the form of a 2 byte unsigned integer (0 - 65535) for each pixel. The data are in the standard Intel (little-endian) binary format.

There were 1016 effective pixels on the linescan camera so the data are stored in lines starting at line 0, pixel 0 to 1015 (2032 bytes) then line 1, pixel 0 to 1015 (2032 bytes) etc. (*_instcnt.conc files have 2032 effective pixels so each data line is twice as long, as explained in Section C.2.)

The concentrations were converted to integers by normalizing the absolute concentration value in mg/l by a MaxC value of 0.4 mg/l and then multiplying by 65534.

$$\text{binary concentration file integer} = \text{integer part of } \left(\frac{C_{\text{measured}}}{\text{MaxC}} \times 65534\right) \tag{45}$$

The MaxC was a slightly higher concentration than could be measured with the linescan laser beam system. Note that this is a different normalization than the method of non-dimensionalizing by the source concentration used in the statistical calculations. The reason this alternative normalization in the data files was simply to conserve storage space. Storing the concentrations as a floating point value or as an integer of sufficient size to accurately express the full range of measured concentrations would have doubled or quadrupled the already large file size.

A value of 65535 (maximum 2 byte unsigned integer) for a pixel indicates that the pixel data point is invalid. Typically, the first 10 and last 10 pixels of each line are excluded from the calculations and given the value of 65535 in the *.conc files. Occasionally other pixels are excluded if they had bad calibration data or were outside the measurement range (below the channel bottom surface in the vertical linescans, for example.) Any further analysis of the concentration data should be sure to exclude values of 65535 from the calculations.

C.3.1 Experiment Configuration Information *_ConcSum.xls

Each array type contains an Excel spreadsheet file with suffix *_ConcSum.xls that contains the following information for each concentration data file. The columns in this file are

concfilename concentration data series file name.

linerate data collection line rate (kHz)

mmperpix width of pixel field of view (mm)

datatime total data collection time (seconds)

srcconc source concentration (mg/l of fluorescein)

srcflow source flow rate (ml/min)

srcx,srcy,srcz source x,y, and z positions in the channel (mm) referenced to the array reference position.

refpix reference pixel for the linescan measurements. For horizontal linescans this is the pixel number at the $y = 0$ reference position for the array. For vertical linescans this is the number of the pixel at $z = 0$ mm (i.e. ground level)

linex x coordinate of line measurement position in the channel (mm)

liney y coordinate of the refpix in the channel (mm) (for vertical profiles liney is the y coordinate of the line measurement position)

linez z coordinate of line measurement position in channel (mm) (for vertical profiles linez is the z position of the refpix)

numpix total number of pixels per line of data

numlines total number of lines collected (datatime*linerate)

MaxC maximum concentration in `*.conc` file (mg/l) i.e. the concentration that is represented by the integer 65534. All concentration measurements in the binary files are normalized by this value.

D Puff Data

For each set of puff releases, several statistics were compiled. As with the continuous releases all measured concentrations were normalized by the source concentration C_{source} so all of the concentration statistics are dimensionless. In all cases, series of 100 puffs were released for each set of puff measurements.

The release sequence for each puff was triggered at time $t = 0$. At time $t = 3$ seconds the 0.5 ml puff of fluorescein dye was released at a rate of 24 ml/min producing a puff duration of 1.25 seconds ending at time $t = 4.25$ seconds. Data were collected for durations of 10,000 line samples at 300Hz up to $t = 33.33$ seconds. There was some uncertainty in the puff start time on the order of ± 0.5 seconds. This was caused by inaccuracies in the pump triggering and in the process used to separate individual puffs from a single data file consisting of many puffs. The release volumes (0.5 ml) and release durations (1.25 s) are very accurate.

Note that each puff must travel downstream to the measurement position, so there delay between the release of the puff and the time at which a measurable concentration appears at the measurement position. The farther downstream the measurement, the longer the delay between the initial release and the appearance of the puff at the measurement position. Series of 100 identical puffs were released for each measurement position.

D.1 Integrated Dose Statistics `*puffdose.csv`

For each pixel in the linescan measurements, an integrated puff dose was calculated by summing the measured concentration over the total duration of each puff measurement.

$$\text{dose} = \sum_{n=1}^{N_{\text{lines}}} c_n \tag{46}$$

where c_n is the normalized dimensionless instantaneous concentration at sample number n, and N_{lines} is the number of sample lines of data collected for each puff. In all cases $N_{\text{lines}} = 10,000$ lines at 300 Hz for a total of 33.333 seconds of data collection per puff released. The units of the dose will be concentration units $\times$ sample time units (i.e. in this study, dimensionless concentration $\times$ 1/300 second). Dose statistics were calculated by evaluating the ensemble properties of the doses from the 100 individual puffs. In the `*puffdose.csv` files the columns of data are:

pixel linescan camera pixel number

mean average dose from the series of puffs.

$$\text{mean} = \frac{1}{N_{\text{puff}}} \sum_{j=1}^{N_{\text{puff}}} \text{dose}_j \tag{47}$$

$$\tag{48}$$

where N_{puff} is the number of puffs.

var variance of dose = $\mathsf{sdev}^2 = \sigma^2_{\mathsf{dose}}$

sdev standard deviation of dose σ_{dose}

$$\sigma_{\mathsf{puff}} = \sqrt{\frac{1}{N_{\mathsf{puff}} - 1} \sum_{j=1}^{N_{\mathsf{puff}}} (\mathsf{dose}_j - \mathsf{mean})^2} \tag{49}$$

$$\tag{50}$$

skew dose skewness

$$\mathsf{skew} = \frac{1}{N_{\mathsf{puff}}} \sum_{j=1}^{N_{\mathsf{puff}}} \left(\frac{\mathsf{dose}_j - \mathsf{mean}}{\sigma_{\mathsf{dose}}} \right)^3 \tag{51}$$

$$\tag{52}$$

kurtosis dose kurtosis

$$\mathsf{kurtosis} = \left[\frac{1}{N_{\mathsf{puff}}} \sum_{j=1}^{N_{\mathsf{puff}}} \left(\frac{\mathsf{dose}_j - \mathsf{mean}}{\sigma_{\mathsf{dose}}} \right)^4 \right] - 3 \tag{53}$$

$$\tag{54}$$

second, third, fourth second, third and fourth moments of dose around zero.

$$\mathsf{second} = \frac{1}{N_{\mathsf{puff}}} \sum_{j=1}^{N_{\mathsf{puff}}} \mathsf{dose}_j^2 \tag{55}$$

$$\mathsf{third} = \frac{1}{N_{\mathsf{puff}}} \sum_{j=1}^{N_{\mathsf{puff}}} \mathsf{dose}_j^3 \tag{56}$$

$$\mathsf{fourth} = \frac{1}{N_{\mathsf{puff}}} \sum_{j=1}^{N_{\mathsf{puff}}} \mathsf{dose}_j^4 \tag{57}$$

D.2 Ensemble Puff Statistics `*enspuffstats.csv`

For selected pixels in the linescans, statistics of the ensemble puffs were calculated for each time step. These results differ from the `*puffdose.csv` files because the results are evaluated for each time step, not integrated over the measurement duration. The columns in the data files are:

time elapsed time from $t = 0$ start of the release sequence, in seconds. At the sampling rate of 300 Hz each time step was $1/300 = 0.00333$ seconds. See the description of the release sequence and timing at the start of Appendix D for clarification on the meaning of elapsed time.

mean ensemble average concentration C

$$\text{mean} = \frac{1}{N_{\text{puff}}} \sum_{j=1}^{N_{\text{puff}}} c_j \tag{58}$$

$$\tag{59}$$

where N_{puff} is the number of puffs.

var variance of puff concentration = $\text{sdev}^2 = \sigma_c^2$

sdev standard deviation of puff concentration σ_c

$$\sigma_c = \sqrt{\frac{1}{N_{\text{puff}} - 1} \sum_{j=1}^{N_{\text{puff}}} (c_j - C)^2} \tag{60}$$

$$\tag{61}$$

skew puff concentration skewness

$$\text{skew} = \frac{1}{N_{\text{puff}}} \sum_{j=1}^{N_{\text{puff}}} \left(\frac{c_j - C}{\sigma_c} \right)^3 \tag{62}$$

$$\tag{63}$$

kurtosis puff concentration kurtosis

$$\text{kurtosis} = \left[\frac{1}{N_{\text{puff}}} \sum_{j=1}^{N_{\text{puff}}} \left(\frac{c_j - C}{\sigma_c} \right)^4 \right] - 3 \tag{64}$$

$$\tag{65}$$

second, third, fourth second, third and fourth moments of puff concentration around zero.

$$\text{second} = \frac{1}{N_{\text{puff}}} \sum_{j=1}^{N_{\text{puff}}} c_j^2 \tag{66}$$

$$\text{third} = \frac{1}{N_{\text{puff}}} \sum_{j=1}^{N_{\text{puff}}} c_j^3 \tag{67}$$

$$\text{fourth} = \frac{1}{N_{\text{puff}}} \sum_{j=1}^{N_{\text{puff}}} c_j^4 \tag{68}$$

D.3 Puff Binary Concentration Files *puff###.conc

Each puff data set has a series of concentration files with the suffix *puff###.conc where ### is the puff number from 000 to 099. The format of the puff concentration files is otherwise identical to the binary concentration files for the continuous releases as discussed in Appendix C.3. Information about the experiment configuration is contained in the *_ConcSum.xls files as described in Appendix C.3.1.

D.4 Puffs with Centroid Meandering Removed

The puff data had the centroid meandering removed using the same methods as described in Section C.2 for the continuous releases. There are complementary ensemble puff statistics files (*_instcntpuffp###enspuffstats.csv), dose statistics files (*_instcntpuffdose.csv) and binary concentration files (*_instcntpuffp###.conc) for the puffs with the centroid meandering removed. In addition, there are files listing the instantaneous centroid and plume spreads for each of the puffs (*puffp###_instcntcntspr.csv).

References

Biltoft, C. A. (2001), Customer Report for Mock Urban Setting Test, Technical Report DPG Document No. WDTC-FR-01-121, Meteorology and Obscurants Division, West Desert Test Center, U.S. Army Dugway Proving Ground, Dugway, Utah.

Coppin, P., Raupach, M., and Legg, B. (1986), Experiments on Scalar Dispersion within a Model Plant Canopy Part II: An Elevated Plane Source, *Boundary-Layer Meteorology*, 35:167–191.

Hinze, J. (1975), *Turbulence*, McGraw-Hill, second edition.

Legg, B., Raupach, M., and Coppin, P. (1986), Experiments on Scalar Dispersion within a Model Plant Canopy Part III: An Elevated Line Source, *Boundary-Layer Meteorology*, 35:167–191.

Press, W. H., Teukolsky, S. A., Vetterling, W. T., and Flannery, B. P. (1992), *Numerical Recipes in C : The Art of Scientific Computing*, Cambridge University Press, second edition.

Raupach, M., Coppin, P., and Legg, B. (1986), Experiments on Scalar Dispersion within a Model Plant Canopy Part I: The Turbulence Structure, *Boundary-Layer Meteorology*, 35:21–52.

DOCUMENT CONTROL DATA

(Security classification of title, body of abstract and indexing annotation must be entered when the overall document is classified)

1. ORIGINATOR (the name and address of the organization preparing the document. Organizations for who the document was prepared, e.g. Establishment sponsoring a contractor's report, or tasking agency, are entered in Section 8.)

Coanda Research and Development Corporation
110A – 3430 Brighton Avenue
Burnaby BC V5A 3H4

2. SECURITY CLASSIFICATION
(overall security classification of the document, including special warning terms if applicable)

Unclassified

3. TITLE (the complete document title as indicated on the title page. Its classification should be indicated by the appropriate abbreviation (S, C or U) in parentheses after the title).

A Laboratory Study of Momentum and Passive Scalar Transport and Diffusion Within and Above a Model Urban Canopy – Final Report

4. AUTHORS (Last name, first name, middle initial. If military, show rank, e.g. Doe, Maj. John E.)

Hilderman, T. and Chong, R.

5. DATE OF PUBLICATION (month and year of publication of document)

December 2007

6a. NO. OF PAGES (total containing information, include Annexes, Appendices, etc) 78

6b. NO. OF REFS (total cited in document) 6

7. DESCRIPTIVE NOTES (the category of the document, e.g. technical report, technical note or memorandum. If appropriate, enter the type of report, e.g. interim, progress, summary, annual or final. Give the inclusive dates when a specific reporting period is covered.)

Final contract report

8. SPONSORING ACTIVITY (the name of the department project office or laboratory sponsoring the research and development. Include the address.)

Defence R&D Canada – Suffield, PO Box 4000, Station Main, Medicine Hat, AB T1A 8K6

9a. PROJECT OR GRANT NO. (If appropriate, the applicable research and development project or grant number under which the document was written. Please specify whether project or grant.)

16QD40

9b. CONTRACT NO. (If appropriate, the applicable number under which the document was written.)

W7702-99R794

10a. ORIGINATOR'S DOCUMENT NUMBER (the official document number by which the document is identified by the originating activity. This number must be unique to this document.)

DRDC Suffield CR 2008-025

10b. OTHER DOCUMENT NOs. (Any other numbers which may be assigned this document either by the originator or by the sponsor.)

CRDC00327

11. DOCUMENT AVAILABILITY (any limitations on further dissemination of the document, other than those imposed by security classification)

(x) Unlimited distribution
( ) Distribution limited to defence departments and defence contractors; further distribution only as approved
( ) Distribution limited to defence departments and Canadian defence contractors; further distribution only as approved
( ) Distribution limited to government departments and agencies; further distribution only as approved
( ) Distribution limited to defence departments; further distribution only as approved
( ) Other (please specify):

12. DOCUMENT ANNOUNCEMENT (any limitation to the bibliographic announcement of this document. This will normally corresponded to the Document Availability (11). However, where further distribution (beyond the audience specified in 11) is possible, a wider announcement audience may be selected).

No limitation on document announcement

13. ABSTRACT (a brief and factual summary of the document. It may also appear elsewhere in the body of the document itself. It is highly desirable that the abstract of classified documents be unclassified. Each paragraph of the abstract shall begin with an indication of the security classification of the information in the paragraph (unless the document itself is unclassified) represented as (S), (C) or (U). It is not necessary to include here abstracts in both official languages unless the text is bilingual).

The objective of the UDM project was to collect extensive data sets of dispersion through groups of obstacles to assist in the development and validation of models of urban dispersion. Both turbulent velocity measurements and scalar concentration data were collected in three different urban obstacle arrays constructed in Coanda's re-circulating water channel: 1. Raupach's 2D tab array; 2. Mock Urban Setting Test (MUST) shipping container; and 3. Urban arrays based on cubical obstacles place in a 2 X 2 unit cell.

In all case, the water channel was configured to simulate rough-surface turbulent atmospheric boundary layer under neutrally stable conditions. Scalar releases were all performed with low momentum sources and neutrally buoyant fluorescent tracer solutions. This report discusses the details of the experiments and provides a brief overview of the data collected. The Appendices give the technical details on the velocity and concentration statistics that were calculated as well as the arrangement of information in the data files.

14. KEYWORDS, DESCRIPTORS or IDENTIFIERS (technically meaningful terms or short phrases that characterize a document and could be helpful in cataloguing the document. They should be selected so that no security classification is required. Identifies, such as equipment model designation, trade name, military project code name, geographic location may also be included. If possible keywords should be selected from a published thesaurus, e.g. Thesaurus of Engineering and Scientific Terms (TEST) and that thesaurus-identified. If it is not possible to select indexing terms which are Unclassified, the classification of each should be indicated as with the title.)

Water channel simulations
Urban flow measurements
Urban dispersion measurements

Defence R&D Canada

Canada's Leader in Defence
and National Security
Science and Technology

R & D pour la défense Canada

Chef de file au Canada en matière
de science et de technologie pour
la défense et la sécurité nationale

www.drdc-rddc.gc.ca